This is an open access article published under an ACS AuthorChoice License, which permits copying and redistribution of the article or any adaptations for non-commercial purposes.

ACS EARTH AND SPACE CHEMISTRY

ACS AUTHORCHOICE

Article

Cite This: ACS Earth Space Chem. 2019, 3, 2017−2032

http://pubs.acs.org/journal/aesccq

Seasonal Flux Measurements over a Colorado Pine Forest Demonstrate a Persistent Source of Organic Acids

S. Ryan Fulgham,[†] Patrick Brophy,[†,∥] Michael Link,[†] John Ortega,[‡] Ilana Pollack,[†,§] and Delphine K. Farmer*[,†]

[†]Department of Chemistry, Colorado State University, Fort Collins, Colorado 80523, United States

[‡]National Center for Atmospheric Research, Boulder, Colorado 80307, United States

[§]Department of Atmospheric Sciences, Colorado State University, Fort Collins, Colorado 80523, United States

Supporting Information

ABSTRACT: Forests can be both sources and sinks of volatile organic compounds to the atmosphere. The role that forests play in controlling organic acid concentrations remains poorly understood with multiple model-measurement comparisons reporting missing sources of formic acid. We conducted seasonal measurements of concentrations and eddy covariance fluxes of oxidized volatile organic compounds over a ponderosa pine forest in Colorado in 2016. Diel concentration profiles show mid-day maxima, consistent with previous studies. We observed persistent but variable upward fluxes of formic, propionic, methacrylic, and butyric acids from the pine forest during all seasons. Formic acid concentrations and fluxes were ∼10 times higher than the other organic acids with daytime exchange velocities on the order of 4−6 cm s^{-1}. The other organic acids had similar exchange velocities as formic acid in the warmer seasons and much smaller exchange velocities in the colder seasons. The upward fluxes for all organic acids increased exponentially with temperature. The observed net upward flux demonstrated that dry deposition was smaller than ecosystem sources of the organic acids. Primary emissions from soil and pine trees were small, in contrast to estimates of in-canopy chemistry. Our study points to an underestimated ecosystem source of organic acids (e.g., in-canopy chemistry of large or multifunctional terpenoids), an overestimated dry deposition sink (potentially due to the arid environment), and/or an unresolved sink of organic acids in the upper boundary layer. Forests are potentially large sources of atmospheric organic acids in warmer seasons but further investigation into dry deposition mechanisms and in-canopy chemistry is warranted.

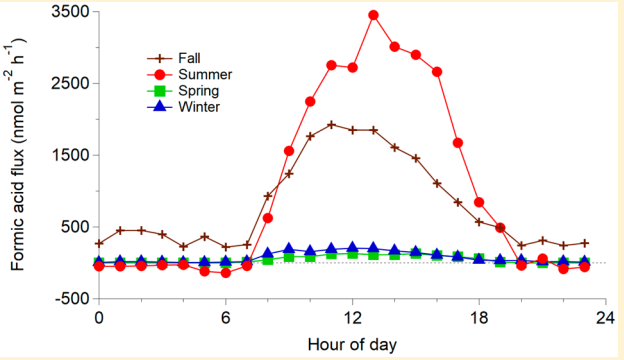

KEYWORDS: *eddy covariance, seasonality, OVOCs, atmospheric budget, biosphere−atmosphere exchange, acetate CIMS*

Downloaded via NOAA CENTRAL LIBRARY on January 26, 2024 at 15:47:38 (UTC).
See https://pubs.acs.org/sharingguidelines for options on how to legitimately share published articles.

1. INTRODUCTION

Organic acids are both numerous and omnipresent in the lower troposphere.[1−6] Organic acids are molecules with one or more carboxylic acid functional groups and may account for ∼25% of nonmethane volatile organic compounds globally in the gas and particle phases.[3] Organic acids can comprise up to 50% of organic aerosol mass, particularly in areas dominated by biogenic emissions.[7,8] This contribution to aerosol loading impacts global climate and air quality and thus human and ecosystem health.[9,10] Organic acids contribute to free acidity and cloudwater acidity and deplete condensed hydroxyl radical (OH) concentrations in clouds.[3,11,12] Their impacts on the carbon cycle, human health, and ecosystem health are well-known but the atmospheric budgets of organic acids are poorly understood. Atmospheric models consistently underpredict measured ambient concentrations of formic acid, suggesting an underestimation of sources and/or an overestimation of sinks.[12−15] Studies of organic acids, other than formic and acetic acids, remain largely unexplored from both modeling and measurement approaches.[16]

Atmospheric organic acids have primary and secondary sources that are both biogenic and anthropogenic. Terrestrial ecosystems provide several primary, biogenic sources of organic acids. Terrestrial vegetation emits formic acid on the order of 2−8 nmol m^{-2} min^{-1} per plant and globally 0.9−6 Tg yr^{-1}.[17−20] Formic, acetic, propionic, butyric, lactic, and keto acids are common volatile products of soil microbes and are emitted from a variety of soils and leaf litters.[21,22] Ants of the Formicinae subfamily are estimated to contribute to global formic acid emissions of 0.6 Tg yr^{-1}.[23] Primary, anthropogenic organic acid sources include a variety of industrial chemical processes and combustion reactions. Secondary oxidation of

Received: June 28, 2019
Revised: July 28, 2019
Accepted: July 29, 2019
Published: July 30, 2019

© 2019 American Chemical Society

DOI: 10.1021/acsearthspacechem.9b00182
ACS Earth Space Chem. 2019, 3, 2017−2032

hydrocarbons is a prolific source of organic acids.[1,12,14,15] Formation reactions include ozonolysis of unsaturated hydrocarbons,[24,25] reactions between stabilized Criegee intermediates and water vapor,[26] and addition of OH to carbonyl groups in the aqueous phase.[11,27] Monoterpene reactions with OH produce short-chain organic acids, including formic, acetic, butyric, and methacrylic acid.[28] Although the chemical mechanisms remain unclear, photooxidation of acetone has been found to be a source of formic acid.[29] Biomass burning is also a source of both organic acids and precursor molecules.[30] Overall, Stavrakou et al. estimate global atmospheric sources of formic acid to be 36 Tg yr^{-1}: 69% biogenic, 11% direct anthropogenic, 8% direct pyrogenic, and 12% indirect anthropogenic and pyrogenic.[15]

Several sinks are known to remove organic acids from the atmosphere. Short-chain, water-soluble organic acids are primarily removed by wet deposition.[16] For example, total organic acids account for 118−244 TgC yr^{-1} lost to wet deposition.[31] Dawson and Farmer derive an average lifetime for formic acid with respect to wet deposition of 5 days.[32] Dry deposition of organic acids is poorly constrained by measurements but is estimated as equivalent to wet deposition.[31] Global formic acid removal rates by dry deposition have been estimated at 12.7−49.5 Tg yr^{-1}, corresponding to a lifetime of 7−14 days.[15] Many short-chain alkanoic acids are relatively inert to atmospheric oxidation. For example, the atmospheric lifetime of formic acid to photochemical oxidation by OH is ∼30 days.[14,33] However, many keto acids, unsaturated acids, and longer-chained organic acids react more favorably with OH.[34] Alkanoic acids, like acetic acid, dominantly react with OH by deprotonation of the acidic hydrogen; similar reactions may also occur for other small alkanoic acids.[35] The multifunctional, oxygenated products of these reactions possess lower volatility and thus efficiently uptake onto particulate matter and cloud droplets.[36]

Model studies incorporate these production and loss processes to investigate the scientific community's understanding of atmospheric organic acids. Most work focuses on formic and/or acetic acids in the summer, consistently finding large discrepancies between model predictions and measurements. Using satellite measurements and a global chemical transport model, Stavrakou et al. find that the standard model misses 100 Tg yr^{-1} of formic acid production worldwide and suggest terpene oxidation is the missing source.[15] Adding isoprene oxidation mechanisms to a global model also underpredicts formic acid, particularly in the northern midlatitudes.[12] Both studies ascribe underpredictions to multiphase chemistry and subsequent loss of formic acid during aerosol aging. Millet et al. add even more formation mechanisms, including formation from stabilized Criegee intermediates and tautomerization of acetaldehyde, to a chemical transport model but still underestimate measurements over a deciduous forest in Alabama.[14] RO_2 + OH reactions pose an intriguing organic acid source but one with such large uncertainty and shallow vertical gradients that these reactions are unlikely the cause of model-measurement discrepancy for formic acid in the boundary layer.[14] As such, Millet et al. show a model-measurement disagreement so large that unrealistic changes to the model are needed to close the discrepancy, for example, increasing isoprene chemistry sources by a factor of 3 or plant emissions by a factor of 26.[14]

Tower-based measurements of ambient organic acids can provide insight into landscape sources and sinks. Canopy-scale eddy fluxes are direct measurements of net vertical exchange over a forest, that is, the difference of local sources and sinks. Several studies have measured organic acid fluxes by direct eddy covariance.[6,13,37−43] Most researchers report bidirectional formic acid fluxes with the bulk of the studies finding net deposition. For example, Alwe et al. found upward fluxes dominated during warm and dry conditions over a mixed-canopy forest, potentially due to in-canopy chemistry.[13] Schobesberger et al. observed large net emissions of formic acid over a boreal forest canopy in Hyytiälä, Finland;[6] observations by Nguyen et al. could account for only half of the expected deposition over an Alabama forest.[40] Mattila et al. noted vertical gradients over a peri-urban site during both daytime and nighttime in Colorado consistent with a surface source of formic acid.[44] These studies point to a large, missing atmospheric source of formic acid.

Previous work has been limited to formic and/or acetic acids, likely due to their prevalence in the atmosphere and ease of calibration. However, organic acids in the atmosphere are diverse, and cover a range of relevant chemical properties (e.g., Henry's Law constant, solubility, vapor pressure).[8,45−49] They present an intriguing opportunity to probe not only ecosystem sources of organic acids but also the potential of chemical properties of gas-phase molecules to control their sinks.

A key challenge in probing sources and sinks of organic acids is the lack of seasonal data coverage. Most published flux measurements are conducted in summer, when plant photosynthetic activity and ecosystem sources are likely at a maximum and are typically limited to days or weeks due to high demand for labor, computational power, and instrument availability coupled with filtering of data for quality assurance. This may lead to an inherent bias in estimates of terrestrial sources and sinks.

To this end, we conducted the Seasonal Particles in Forests Flux studY (SPiFFY), with the aim of investigating interactions between semivolatile organic compounds and particle fluxes over a subalpine forest across multiple seasons. Here, we present seasonally representative eddy covariance flux measurements of six organic acids: formic, propionic, methacrylic, butyric, valeric, and heptanoic acids from a ponderosa pine forest where total VOCs are dominated by monoterpene and 2-methyl-3-buten-2-ol (MBO) emissions. To constrain primary sources of the six organic acids, we measured direct emissions of the acids from pine trees and soils with branch and soil enclosures. We reproduce observed fluxes via implementing temperature-dependent parametrizations. Finally, we construct flux budgets for the six acids to explore the relative importance of different sources and sinks for the organic acids across the seasons.

2. SITE DESCRIPTION

SPiFFY consisted of four, seasonally representative intensive measurement campaigns at the Manitou Experimental Forest Observatory (MEFO): winter (February 1−March 1, 2016), spring (April 15−May 15, 2016), summer (July 15−August 15, 2016), and fall (October 1−November 1, 2016). A preliminary summer campaign took place in 2015 (July 1 −August 15, 2015) and was used to pilot these experiments; however, only measurements from the 2016 campaign that were optimized for data collection in this environment are utilized in this analysis. Manitou Experimental Forest Observatory (39.1006°N, 105.0942°W) is an atmospheric observation station located in central Colorado, U.S.A. Semiarid, subalpine

DOI: 10.1021/acsearthspacechem.9b00182
ACS Earth Space Chem. 2019, 3, 2017−2032

Table 1. Seasonal Averages ±1 Standard Deviation of Environmental Conditions at MEFO (Measurements Taken at 27.8 m a.g.l.)[a]

		relative humidity %	temperature °C	wind speed (m s^{-1})	wind direction (°)	PPFD (μmol m^{-2} s^{-1})
		$\mu \pm \sigma$ (min−max)	$\mu \pm \sigma$ (min−max)	$\mu \pm \sigma$ (min−max)	μ	$\mu \pm \sigma$ (min−max)
winter	day	27 ± 10 (8.0−88)	7 ± 5 (−7.0−16)	3.5 ± 2 (0.25−11)	314	210 ± 300 (0.0−1000)
	night	43 ± 20 (15−89)	0 ± 5 (−13−11)	2.7 ± 1 (0.22−6.9)	154	
spring	day	40. ± 20 (0.0−93)	10 ± 6 (−3.7−21)	3.6 ± 2 (0.0−18)	279	280 ± 400 (0.0−1300)
	night	64 ± 20 (0.0−93)	3 ± 5 (−8.1−18)	2.3 ± 1 (0.0−10)	161	
summer	day	33 ± 20 (0.0−86)	23 ± 4 (11−29)	3.0 ± 1 (0.0−10)	119	330 ± 400 (0.0−1200)
	night	64 ± 20 (7.0−91)	14 ± 3 (5.7−29)	2.2 ± 1 (0.10−10)	145	
fall	day	25 ± 10 (0−92)	15 ± 4 (0.5−23)	3.4 ± 2 (0.0−11)	343	290 ± 400 (0.0−1200)
	night	47 ± 20 (13−92)	6 ± 5 (−7.1−20)	2.4 ± 1 (0.20−12)	146	

[a]Seasonal maxima and minima are in parentheses. Daytime hours are taken as 8:00−18:00 local time, and nighttime hours 19:00−7:00. PPFD is measured at the U.S. Forest Service main office (~2 km east of the site) and includes down-welling solar radiation at 3 m a.g.l.

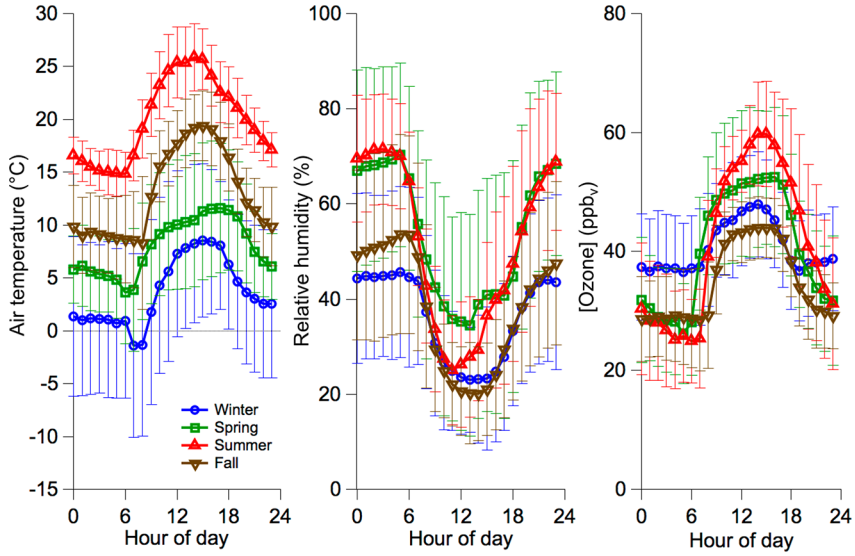

Figure 1. Seasonally averaged temperature (left), relative humidity (center), and ozone mixing ratios (right) during the measurement campaigns vary across the seasons. Points represent hourly averages with error bars encompassing ±1 standard deviation. Hours of day are derived from local time, which we define as Mountain Daylight time (UTC −6) for spring, summer, and fall seasons and Mountain Standard time (UTC −7) for the winter season.

(2280−2840 m above sea level) Rocky Mountain ponderosa pine forest surrounds the site to the north, south, and west. Ortega et al. provide a detailed description of both the site and forest.[50] Average canopy height at the measurement location was approximately 16 m with sparse coverage. Various herbaceous and woody plants grew in the understory. Approximately 1 km to the east of MEFO is a creek drainage and Colorado state highway 67. The two-lane highway typically experienced light traffic from recreational vehicles, forest workers, and local residents.

Seasonal meteorology is summarized in Table 1. Temperature changed substantially between seasons: −1 ± 8 °C (mean ± standard deviation) in winter, 4 ± 7 °C in spring, 20 ± 7 °C in summer, and 8 ± 8 °C in fall. The maximum recorded temperature (30 m above ground level, a.g.l.) during our study was 30 °C (July 17, 2016), and the minimum recorded temperature (30 m a.g.l.) was −22 °C (February 3, 2016). Means of relative humidity range from 50 to 70% for all seasons. Nighttime relative humidity rarely exceeded 80%; daytime relative humidity seldom falls below 20%. Seasonal variability in ambient temperature and relative humidity is shown in Figure 1. Consistent with previous observations at the site, daytime winds predominantly traveled from north to south.[50] At night, above-canopy winds drained toward the north. Average wind speeds (30 m a.g.l.) were light to gentle-moderate (<4.0 m s^{-1}). Total annual rainfall at the site was 30 cm in 2016.[51] Light afternoon thunderstorms frequently occurred in summer, with cumulative precipitation of 2 cm during the summer campaign. Light snowfall (<10 cm total precipitation) occurred at the beginning of October 2016, otherwise the fall campaign was devoid of precipitation. Two substantial snowstorms (>30 cm accumulation per event) happened during both winter and spring (February 3−4 and 23, 2016, April 15−16, 2016, and April 28−May 1, 2016). Most of the snow cover melted between storms. Characteristic of the Colorado Front Range, sunny days persisted at Manitou. Down-welling photosynthetic photon flux density (PPFD) at 3 m a.g.l. regularly exceeded 1000 μmol m^{-2} s^{-1} during all seasons characterized in this work.

We installed sonic anemometers and inlets for flux measurements on the 30 m walk-up "chemistry" tower at the Manitou site with instruments housed in a nearby mobile trailer. We also collected measurements of nitrogen oxides (NO_x = NO + NO_2), ozone (O_3), carbon monoxide (CO), and sulfur dioxide (SO_2) during these seasonal experiments. Descriptions for these measurements are in Supporting

DOI: 10.1021/acsearthspacechem.9b00182
ACS Earth Space Chem. 2019, 3, 2017−2032

Information (S2). Section 4 contains details of the estimated flux footprint.

3. MEASUREMENTS

3.1. Organic Acid Measurements. We measured gaseous formic {HCOOH}, propionic {CH_3CH_2COOH}, methacrylic {$CH_3C(CH_2)COOH$}, butyric {$CH_3(CH_2)_2COOH$}, valeric {$CH_3(CH_2)_3COOH$}, and heptanoic acids {$CH_3(CH_2)_5COOH$} with an acetate high-resolution time-of-flight chemical ionization mass spectrometer (hereafter referred to as CIMS; Tofwerk AG and Aerodyne Research, Inc.). We used acetate reagent ions throughout SPiFFY except during 5 days in summer and 3 days during fall when we used iodide reagent ion chemistry. This manuscript focuses only on acetate CIMS data. The sensitivity of acetate CIMS does not substantially depend upon ambient water vapor concentrations unlike I^-, CF_3O^-, and H_3O^+ CIMS, which have typically been used for previous flux measurements. Importantly, we note that while acetate CIMS cannot distinguish between structural isomers, the technique has little sensitivity to most other functional groups, so we relate signals to their most likely detected structures (i.e., carboxylic acids). However, some of these structures do have multiple structural isomers that maintain the acidic functionality. For example, we detect the deprotonated product of $C_4H_8O_2$, which represents the sum of butyric and isobutyric acid (hereafter referred to as "butyric acid" for simplicity); other isomers, such as acetoin, do not possess adequately acidic hydrogen atoms for detection by acetate reagent ions. Similarly, $C_7H_{14}O_2$ (hereafter referred to as "heptanoic acid" for simplicity) represents the sum of all C_7-alkanoic acids. Both CIMS and acetate ionization mechanisms are described thoroughly elsewhere and are briefly described here.[52−55]

In this technique, sample air enters the ion−molecule reactor (IMR, 70 mbar) and mixes with an orthogonal stream of acetate reagent ions. Acetate reagent ions are thought to initially cluster in the IMR and then decluster in the atmospheric pressure interface to produce declustered, deprotonated analyte ions further downstream in the CIMS.[53] Ionized analytes pass through both short and big segmented, RF-only quadrupoles before entering a series of ion transfer lenses. A voltage drop of 19 V between the ion lenses (skimmer and second quadrupole entrance plate) keeps the CIMS in a declustering mode, minimizing the detection of acetate−analyte clusters. After transmission, sample ions are orthogonally extracted, separated, and detected in the time-of-flight (ToF) region. Signal from the microchannel plate detector (Photonis Inc.) is amplified by 11 times, preaveraged on an analog-to-digital converter (ADQ 1600, SP Devices), transferred to a computer (Dell Technologies, Inc.) by USB 2.0, and extracted at 15 kHz into the data acquisition system (ToFDAQ). All measurements are averaged to 5 Hz time resolution. Mass resolutions $>3.5 \times 10^3$ ($m/\Delta m$) and total counts $>8 \times 10^5$ ions per spectrum are maintained during winter, spring, and the first 2 weeks of summer, at which point instrument sensitivity dropped to 2×10^5 ions per spectrum for the duration of the study.

A reduced pressure inlet (Figure S1), similar to that described by Brophy and Farmer, samples air, although a durable perfluoroalkoxy alkane (PFA) inlet replaces the glass inlet.[52] Gases and particles enter a 1/4 in. PFA three-way tee (Swagelok) and flow through 11 cm of 1/8 in. i.d. (1/4 in. o.d.) fluorinated ethylene propylene (FEP) tubing. The flow is split with a sample bypass flow (40 L min^{-1}, volumetric flow; 30 L min^{-1}, standard flow), removing gases orthogonally from the main flow line with the aim of minimizing particle interferences, and a particle bypass flow (10 L min^{-1}), pulling additional sample air through the inlet. Both flows are pumped by a single Triscroll 600 pump (Varian, Inc.). Gas sample moves from the inlet through 30 m of 3/8 in. i.d. (1/2 in. o.d.) FEP and tubing diameter reduces to 1/8 in. i.d. (1/4 in. o.d.) with a Swagelok reducing union. Finally, the CIMS subsamples at 4.5 L min^{-1}. A PFA three-way tee positioned between the sample bypass line and IMR enables calibration gas addition (described below). The remaining sample bypass air flow recombines with the particle bypass flow, modulated by an inlet flow and pressure control box. Particle bypass and sample bypass flows are each measured by analog mass flow meters (MKS Instruments, model 179) prior to recombination. After recombining the particle bypass and sample bypass lines in the inlet box, a Baratron pressure transducer (MKS Instruments, model 750) monitors pressure, which we maintain at 350 mbar with a fast-acting, bidirectional needle valve (Aalborg Instrument and Controls, Inc., model SMV20-SVD2-A) and a PID loop automated with LabVIEW (National Instruments Corporation).

The inlet system described above is designed to minimize differences in sampling residence times for different measured species (e.g., reduced inlet and sampling line pressure). We find little influence of the long tubing length for the inlet from the tower on instrument time response owing to turbulent flow in the inlet line (e.g., Reynold's numbers of >4000 for this sampling system). The residence time in the inlet tubing between the inlet tip at the top of the tower and the CIMS inside the trailer is 3 s. This is a similar to the lag-covariance time of 4 s determined for the segment of tubing between the sonic anemometer and the CIMS detector (Figure S2). Emission peaks for all acids occur at or very close to zero lag-time lending confidence to the use of one lag time for multiple organic acid fluxes. Additionally, signal peaks at zero lag time clearly emerge from background noise evident at positive and negative lag times. We evaluated the response time of the system at MEFO by overflowing the inlet at the top of the tower with UZA and waiting for the detector signal to fall to zero. The resultant signal-decays from ambient concentrations are fit well by a single exponential decay function with e-folding times ranging from 0.59−4.6 s for calibrated organic acids. Formic acid e-folding times are similar regardless of UZA overflow location (2.9 s at inlet on top of tower versus 2.7 s at CIMS inlet in ground trailer), suggesting that most wall interactions happen in the ion−molecule reaction chamber of the CIMS (Figure S3). Previous measurements of other VOCs and OVOCs typically ignore potential dampening effects in high-frequency signal fluctuations due to wall interactions. Such interactions are known to occur and cause delays in response time in even short segments of Teflon tubing on the order of seconds and up to several minutes for low volatility compounds.[56] Further, spectral analysis suggests little dampening in the sampling lines (Section 4). Thus, we ignore attenuation due to wall interactions for the volatile organic acids described herein.

The CIMS was calibrated online once every 1−2 h using an automated calibration source. Calibrations included standard additions of formic, propionic, methacrylic, and butyric acids during all seasons; external standards of formic acid during winter and spring; and standard additions of valeric and

DOI: 10.1021/acsearthspacechem.9b00182
ACS Earth Space Chem. 2019, 3, 2017−2032

heptanoic acids during summer and fall. System blanks were performed during every calibration period. Section S1 provides details of the calibration timeline and sample data.

We process CIMS data according to standard practices using ToFware version 2.5.7. Prior to high-resolution peak fitting, CIMS signals (mV ns s^{-1}) are baseline corrected and converted to counts s^{-1} by normalizing with a single-ion signal. We mass calibrate CIMS data using ≥10 fully resolved ions known to be in the spectrum m/z 32−283 (CHO_2^-, $C_2H_3O_2^-$, NO_2^-, NO_3^-, I^-, Cl^-, O_2^-, $C_{12}H_{23}O_2^-$, $C_{13}H_{25}O_2^-$, $C_{14}H_{27}O_2^-$, $C_{15}H_{29}O_2^-$, $C_{16}H_{31}O_2^-$, $C_{18}H_{35}O_2^-$, CF_3^-, $C_2F_3O_2^-$, and $C_{12}H_3Cl_4O^-$). We identify and fit peaks based on exact peak masses and established rules of covalent bonding. The resulting peak areas are normalized by total acetate ion signal area and multiplied by the total ion signal area measured during system blanks. We calculate mixing ratios of the six organic acids for which we have permeation standards by subtracting backgrounds (system blank) and dividing by immediately preceding bihourly sensitivities. Calibration periods take approximately 15 min. In preparation for eddy covariance analysis, we truncate each time series into one, 30 min continuous flux period and realign the mixing ratio time series forward by 4 s to account for offsets in time between acquisition of CIMS and wind speed data (Figure S2). We thus report one 30 min average value of flux per species per hour.

The CIMS was coupled to a branch enclosure during summer and soil chambers during fall to constrain direct emissions of organic acids from ponderosa pine and soils, respectively. Supporting Information Section S2.1 contains details of these measurements systems.

3.2. Sonic Anemometer. A Windmaster Pro sonic anemometer (Gill Instruments Limited, Lymington, U.K.) mounted 30 m a.g.l. measures three-dimensional wind speed vectors and temperature. Data are transmitted via RS-422 and logged at 5 Hz time resolution with ToFDAQ data acquisition software (Tofwerk AG). The anemometer model requires a firmware correction affecting vertical wind speeds (w). Positive w values +16.6% and negative w values +28.9% are corrected according to the manufacturer's specifications.[57] We flag spikes in anemometer data with a median absolute deviation filter following the methods described in Mauder et al.[58] Flagged values are replaced by linear interpolation unless >10 consecutive flags are found in which case the entire flux period is removed from subsequent analysis. We flagged less than 0.5% of points from each wind vector or temperature time series. We rotate wind vectors to a natural coordinate system by double rotation before trimming the time series to match the CIMS data flux periods in preparation for eddy covariance calculations.[59]

4. EDDY COVARIANCE CALCULATIONS

We calculate the vertical flux of each of the six organic acids by the eddy covariance method. Eddy covariance fluxes are quasi-continuous and represent a spatially integrated footprint.[60] We calculate the flux between the surface and point of measurement for each flux period from the appropriately lagged 5 Hz mixing ratio (or temperature for sensible heat flux) and vertical wind speed data by eq 1

$$F = \overline{w'C'} \tag{1}$$

where F is the vertical flux (ppt_v m s^{-1}, which can be converted to nmol m^{-2} h^{-1}, or °C m s^{-1}, which can be converted to W m^{-2}), C is the mixing ratio (ppt_v) (or temperature (°C)), w is vertical wind speed (m s^{-1}), and $'$ refers to instantaneous deviations from the 30 min mean. We note that at MEFO during SPiFFY 1 ppt_v m s^{-1} is on average equivalent to 107.5 nmol m^{-2} h^{-1}. All fluxes are reported as nmol m^{-2} h^{-1}. The sign convention is such that a positive flux value represents an upward flux from the surface to the atmosphere. A negative flux value represents a downward flux from the atmosphere toward the surface. We do not correct the calculated CIMS fluxes with temperature heat spectra due to the lack of substantial, high-frequency spectral attenuation (<1% of total flux) in organic acid cospectral analyses. Because the sample line pressure is controlled for constant pressure, we do not apply the Webb−Pearman−Leuning correction.[61] Relative humidity corrections are applied to neither flux, nor concentrations as the instrument sensitivity for acetate CIMS has a negligible dependence on water vapor at the relative humidity ranges observed at MEFO.[53] Horizontal sensor separation between the sonic anemometer and inlet is also negligible. We investigate each flux period to ensure that data meet three key assumptions. Any flux period that fails a test is removed from subsequent analysis.

(1) Turbulence at the measurement height must be well-developed. Friction velocity (u*) is a measure of horizontal wind shear forces, which is closely linked to atmospheric stability. Here, turbulence is considered to be well-developed when u* > 0.14 m s^{-1}. We apply u*-filtering to exclude flux periods for which advection may yield spurious fluxes. Several studies have tabulated u* thresholds for various types of environments, finding that minimum u* thresholds for forested sites vary between 0.1−0.15 m s^{-1}.[62−64] Values of 84%, 78%, 79%, and 77% of the data pass the turbulence test in winter, spring, summer, and fall, respectively.

(2) Fluxes must remain in steady state within the 30 min flux period. A stationarity test determines the mean of six consecutive 5 min segments relative to the full 30 min flux period; flux periods are considered to pass when the deviation is <30%.[65] Values of 39−66%, 38−51%, 89−93%, and 43−65% of the data meet the stationarity criterion in winter, spring, summer, and fall, respectively.

(3) During the fall, the United States Forest Service conducted several prescribed burns to thin vegetative detritus from forest floors. The burns include a large, adjacent parcel of forest to MEFO. To exclude biomass burning contributions from organic acid measurements in the fall, flux periods with observable CO spikes in the time series are excluded. Values of 98% and 100% of data pass CO filtering in fall and other seasons, respectively.

Overall, 36−62%, 35−46%, 4−48%, and 36−58% of flux periods during winter, spring, summer, and fall, respectively, meet quality control criteria described above (ranges represent the different organic acid analytes: formic acid most frequently passed the filters, heptanoic acid least frequently). Eighty-two percent of the daytime data and 49% of the nighttime flux periods meet the quality control criteria described above for formic acid. Heptanoic acid fails to meet quality control criteria during all summer flux periods.

Fluxes represent the pine forest fetch. We calculate footprints for each season using a canopy height of 16 m and displacement height of 10.7 m.[66] Under stable conditions (Monin-Obukhov length (L) > 0), 90% flux contours are long, >2000 m north−south, and narrow, >1000 m east−west. Unstable footprints (L < 0) are more evenly distributed,

DOI: 10.1021/acsearthspacechem.9b00182
ACS Earth Space Chem. 2019, 3, 2017−2032

Table 2. Seasonal Averages ± Standard Deviations of Organic Acid (Parts Per Trillion by Volume, ppt_v) and Trace Gas (Parts Per Billion or Parts Per Million by Volume, ppb_v or ppm_v) Mixing Ratios at MEFO[a]

	winter	spring	summer	fall
	$\mu \pm \sigma$ (min−max)	$\mu \pm \sigma$ (min−max)	$\mu \pm \sigma$ (min−max)	$\mu \pm \sigma$ (min−max)
CH_2O_2 (ppt_v)	55 ± 57 (below detection limit − 950)	30 ± 24 (b.d.l. − 150)	1200 ± 910 (66−8600)	810 ± 480 (86−5200)
$C_3H_6O_2$ (ppt_v)	3.5 ± 1.7 (b.d.l. − 25)	2.0 ± 1.0 (b.d.l. − 11)	63 ± 44 (b.d.l. − 380)	29 ± 18 (b.d.l. − 170)
$C_4H_6O_2$ (ppt_v)	0.43 ± 0.20 (b.d.l. − 9.2)	0.30 ± 0.14 (b.d.l. − 2.8)	10. ± 8 (b.d.l. − 140)	4.2 ± 2.6 (b.d.l. − 27)
$C_4H_8O_2$ (ppt_v)	1.1 ± 0.7 (b.d.l. − 22)	0.88 ± 0.59 (b.d.l. − 7.4)	45 ± 29 (b.d.l. − 250)	12 ± 9 (b.d.l. − 87)
$C_5H_{10}O_2$ (ppt_v)	n/a	n/a	13 ± 9 (b.d.l. − 85)	6.3 ± 5.4 (b.d.l. − 59)
$C_7H_{14}O_2$ (ppt_v)	n/a	n/a	15 ± 13 (b.d.l. − 210)	9.7 ± 9.4 (b.d.l. − 140)
O_3 (ppb_v)	41 ± 10 (0.40−84)	41 ± 14 (1.5−82)	41 ± 16 (1.1 − 97)	35 ± 9.2 (4.0−60.)
NO_x (ppb_v)	n/a	n/a	1.4 ± 0.9 (0.42 − 6.9)	1.2 ± 1.4 (b.d.l. − 8.1)
SO_2 (ppb_v)	n/a	n/a	0.60 ± 0.34 (b.d.l. − 2.8)	0.36 ± 0.30 (b.d.l. − 1.6)

[a]Seasonal maxima and minima are in parentheses. Daytime hours are 8:00−18:00 local time. Nighttime hours are 19:00−7:00.

Table 3. Percentage of Organic Acid Fluxes (F_{acid}) That Exceed Corresponding Flux Detection Limits (F_{unc}) during Each Season (See Text for Details of Calculation)[a]

	percentage (%) of flux periods in which $F_{acid} > F_{unc}$ (daytime, nighttime)					
season	formic	propionic	methacrylic	butyric	valeric	heptanoic
winter	68 (89, 51)	16 (25, 9)	9.0 (14, 5)	26 (42, 14)	n/a	n/a
spring	68 (90, 49)	35 (52, 20)	17 (22, 13)	45 (69, 24)	n/a	n/a
summer	65 (86, 46)	40 (53, 29)	27 (41, 16)	47 (68, 28)	40 (55, 26)	23 (37, 11)
fall	64 (92, 40)	21 (35, 9)	12 (16, 8)	29 (48, 11)	19 (29, 11)	10 (14, 6)

[a]Fluxes in parentheses separate the percentages of qualifying flux periods between daytime (8:00−18:00; left) and nighttime (19:00−7:00; right). The CIMS was not calibrated for valeric and heptanoic acids in winter and spring, therefore fluxes for these acids during cold seasons are not available (n/a).

extending >400 m in all directions (Figure S4). Although many footprints include Colorado Highway 67, 1 km east of MEFO, we find no statistical difference in the distribution of organic acid fluxes when flux periods including the highway are excluded. We exclude no flux periods on the basis of footprints.

During flux periods with low turbulence, trace gases can be stored in canopy air, particularly in canopies with dense foliage, which inhibit eddy penetration. Without vertical gradient measurements of organic acids, we do not estimate the storage term during any season at SPiFFY. However, a previous organic acid eddy flux study over a boreal forest (Leaf Area Index (LAI) = 6.3) determined the storage term for formic and acetic acids to be negligible. The canopy at MEFO is less dense (LAI = 1.14) allowing more penetration of eddies carrying organic acids.[39] More importantly, organic acid flux data is filtered to exclude flux periods with low turbulence, in which canopy storage of trace gases is more pronounced. We thus ignore the storage term for organic acid fluxes in this work.

We use spectral analysis to investigate the quality of CIMS flux measurements. Co-spectral densities of vertical wind speed and mixing ratio represent the organic acid flux as a function of frequency, a proxy for eddy size. Average cospectral densities (Figure S5) are calculated for all organic acids during each season between 9:00 and 15:00 local time. Here, "local time" refers to Mountain Daylight time (UTC −6) during spring, summer, and fall campaigns and Mountain Standard time (UTC −7) during the winter campaign. Cospectra of temperature flux (sonic temperature and vertical wind speed) are similar to organic acid cospectra, demonstrating that high frequency variations are not significantly attenuated by the inlet at frequencies <2.5 Hz. Averaging times are long enough, time resolutions fast enough, and organic acids detection sufficiently sensitive to observe an inertial subrange in the spectra for all acids. We hypothesize that reducing and controlling inlet pressure in the closed-path system obviates the need for spectral transformation. We note that substantial spectral attenuation may occur at frequencies >2.5 Hz; however, frequencies beyond the Nyquist frequency (2.5 Hz here) are obfuscated by aliasing.

Time-lagged covariance functions between vertical wind speeds and mixing ratios of organic acids provide a useful calculation of uncertainty in eddy covariance fluxes. The covariance at lag times far exceeding the flux integral time scale represent the combined random instrument noise and environmental fluctuations that contribute to measured fluxes.[67,68] We calculate the flux detection limit for an individual organic acid for a single flux period as 3σ of covariances lagged 30−60 s in both positive and negative directions. Observed fluxes of formic acid consistently exceed the detection limit for two-thirds of the flux periods, while observed methacrylic acid fluxes were often below detection limit (Table 3). More daytime fluxes exceeded detection limit than nighttime fluxes.

5. RESULTS

MEFO experienced clean continental air with occasional intrusions of polluted, urban air from Denver or Colorado Springs. SO_2 concentrations are generally below 1 ppb_v but spike above 1.5 ppb_v during some evenings when winds are northeasterly or southeasterly (i.e., from Front Range cities). NO_x concentrations trend similarly with wind direction at MEFO and are consistent with past measurements. Ozone rarely exceeds 60 ppb_v even during peak photochemistry in the summer. The ozone maximum was 97 ppb_v on 28 July. Seasonal measurements of trace gases, including organic acids, are summarized in Table 2.

MEFO is similar to other coniferous forest sites in terms of formic acid concentrations. Daytime formic acid at MEFO

DOI: 10.1021/acsearthspacechem.9b00182
ACS Earth Space Chem. 2019, 3, 2017−2032

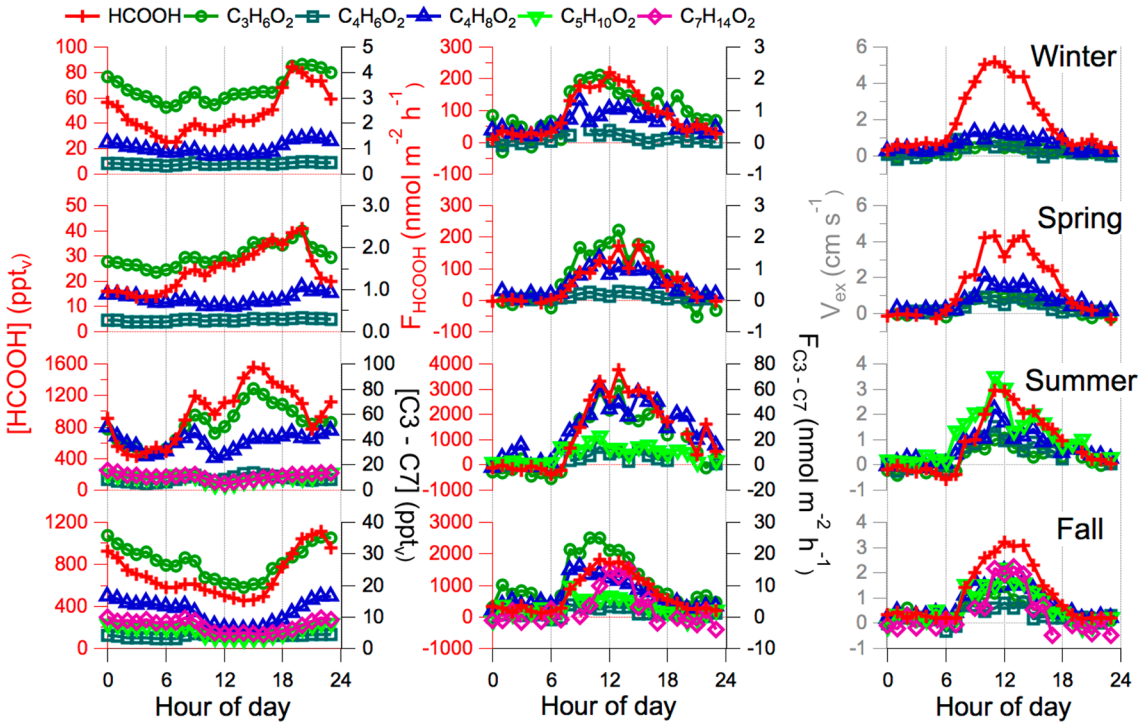

Figure 2. Seasonal diel mixing ratios (ppt_v, left), fluxes (nmol m^{-2} h^{-1}, middle), and exchange velocities (cm s^{-1}, right) for six organic acids. Data points represent seasonal, hourly medians. Fluxes and exchange velocities are filtered according to Section 4. From top to bottom, seasons are winter, spring, summer, and fall. For mixing ratio and flux plots, formic acid mixing ratio is on the left axis, and propionic, methacrylic, butyric, valeric, and heptanoic acids are on the right axis. Upward fluxes and exchange velocities are evident for all organic acids during the daytime with average nighttime fluxes approaching zero. See Figures S9–S14 for additional details.

peaked at 2–6 ppb_v in the summer, comparable to peak observations (2–3 ppb) over a boreal forest in Finland during summer 2015.[6]

Formic acid mixing ratios are 10–100 times higher than other organic acids. Mixing ratios for all organic acids are an order of magnitude higher in warmer seasons (summer and fall) than in colder seasons (winter and spring). All six organic acids follow the same diel trends within a given season. In the summer, organic acids increase at sunrise, reach a late afternoon or evening maximum, and then decrease overnight in all seasons (Figure 2). A midmorning (~9:00 local time) reduction in all organic acid mixing ratios occurs most days and is consistent with the breakup of the nocturnal boundary layer. Formic, propionic, butyric, and valeric acids follow the same diel trends as previous measurements in the Colorado Front Range, although summer formic acid at the Boulder Atmospheric Observatory is about a factor of 2 higher than at MEFO.[44]

Organic acid fluxes are consistently upward throughout all four seasons. We note that though this paper focuses on small organic acids, other compounds, such as isocyanic acid, exhibit downward fluxes, which will be the focus of future publications. This indicates persistent ecosystem sources of all six organic acids (Figure 2). Diel cycles in flux differ from concentration. Fluxes increase from near-zero at sunrise and peak at mid-day before decreasing back to zero (within measurement uncertainty) near sunset. Downward organic acid fluxes are rare, accounting for only 6–15% of all unfiltered fluxes and 1–8% of all quality-filtered fluxes exceeding the flux detection limit. Most (>99%) downward flux events occurred at nighttime. Organic acid fluxes are approximately an order of magnitude lower in winter and spring than in summer and fall.

We calculate exchange velocity (V_{ex}, cm s^{-1}) as the flux divided by the average concentration of the flux period for each acid. Positive exchange velocities represent emission rates from the forest, whereas negative exchange velocities represent deposition rates. V_{ex} provides a flux normalized by concentration, thus enabling comparison of biosphere–atmosphere exchange rates across different sites subject to different concentration regimes. V_{ex} is equivalent in magnitude to deposition velocity (V_{dep}) but opposite in sign convention ($V_{ex} = -V_{dep}$). V_{ex} is commonly used to denote the average vertical rate of exchange between the measurement height and the surface, particularly for eddy flux measurements of oxygenated volatile organic compounds.[6,13,37,40,69−71] Despite formic acid having orders of magnitude higher concentration than the other organic acids, the exchange velocities are all of the same order of magnitude in the spring and summer. In contrast, during the colder spring and winter months, formic acid emission rates are again much higher than the other acids, indicating that the fluxes may be driven by different processes for the different organic acids.

6. DISCUSSION

The observed organic acid mixing ratio and flux diel cycles require a daytime source coupled to a rapid (i.e., lifetime of hours) sink. Summer observations are similar to previous studies: mixing ratios peak in the mid-day, similar to summertime measurements in forests[2,40,72] and urban sites.[49] The upward formic acid flux maximizes in the middle of the day, similar to formic acid flux observations at Hyytiälä.[6]

Large canopy-level emissions at MEFO indicate that formic acid is potentially an important source of reactive atmospheric carbon. In summer 2010, Kaser et al. measured 0.50 mg m^{-2}

DOI: 10.1021/acsearthspacechem.9b00182
ACS Earth Space Chem. 2019, 3, 2017−2032

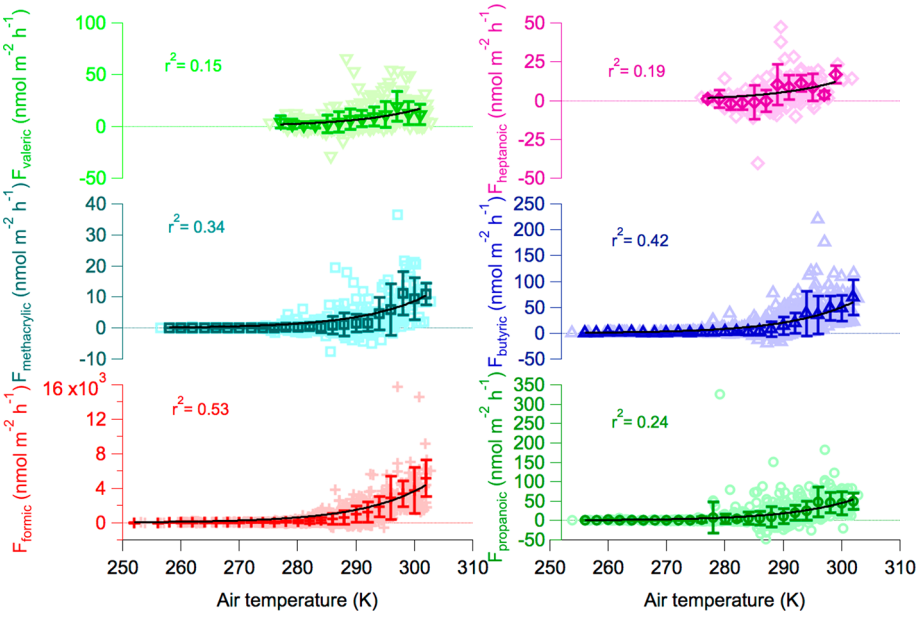

Figure 3. Organic acid fluxes increase with ambient air temperature at MEFO. The black lines represent an exponential fit of the form, $F_{net} = F_{std}e^{0.09(T-303)}$ (see eq 2), where F_{net} is the quality-filtered canopy flux, F_{std} is standard emission at 303 K, and T is the temperature separated into 2 K bins (all seasons). Error bars represent the standard deviation of each bin. We determine correlation coefficients (r^2) for the model versus the observational data. Winter and spring data are absent for valeric and heptanoic acids due to the lack of calibrations during those seasons.

h^{-1} (37 μmolC m^{-2} h^{-1}) mid-day average monoterpene emission fluxes that were only 10 times larger than summer 2016 mid-day median formic acid fluxes of 3.8 μmolC m^{-2} h^{-1}.[39]

Despite measuring a sizable range of organic acid concentrations across the seasons, we observe no evidence of a compensation point (i.e., no consistent shift from emission to deposition as ambient concentrations increase), contrary to observations over a tropical forest by Jardine et al. (Figure S7).[37]

The upward organic acid fluxes persist through the seasons. Compiling the data demonstrates that organic acid fluxes increase exponentially with temperature (Figure 3) and vapor pressure deficit (Figure S8), decrease exponentially with relative humidity but do not correlate with photoactive photon flux density (PPFD) (r^2 < 0.10 for formic acid) or O_3 (r^2 < 0.15). These correlations initially appear consistent with a direct plant source of the organic acids to the atmosphere but closer inspection reveals evidence for other sources.

The strong temperature dependence of the observed organic acid fluxes follows the exponential temperature equation used by ecosystem emissions models for light independent plant VOC emissions. For example, the Model of Emissions of Gases and Aerosols from Nature (MEGAN)[73] models monoterpene fluxes as

$$E = E_f e^{\beta(T-T_s)} \quad (2)$$

where E_f is the basal emission rate (nmol m^{-2} h^{-1}) at a standard temperature (T_s, 303 K), T is the ambient temperature in Kelvin, and β represents a temperature scaling factor, assigned a value of 0.09 K^{-1} for monoterpenes, which sets the emission to E_f at T_s. We fit the canopy-level flux data from all seasons to eq 2 to derive E_f and calculate basal emission rates of 4700 ± 210 nmol m^{-2} h^{-1} for formic, 59 ± 3.2 nmol m^{-2} h^{-1} for propanoic, 12 ± 0.9 nmol m^{-2} h^{-1} for methacrylic, 66 ± 3.2 nmol m^{-2} h^{-1} for butyric, 20 ± 2.2 nmol m^{-2} h^{-1} for valeric, and 17 ± 3.2 nmol m^{-2} h^{-1} for heptanoic acids. The model accounts for only 15−53% of the variance of the organic acid fluxes.

Nighttime fluxes are particularly problematic as nocturnal temperatures are high enough to result in a much larger predicted nighttime emission than the near-zero flux we observed. Of course, this analysis ignores contributions of dry deposition to the observed flux, which could improve model-measurement agreement. Incorporating light into the model, as with the Parameterized Canopy Environment Emission Activity (PCEEA) model, provides a better representation of the diel cycle than the temperature-only MEGAN model but underestimates daytime upward fluxes and fails to improve the correlation coefficients (r^2 = 0.15−0.53 for temperature only; 0.24−0.50 for temperature and light).[74] The weak correlation coefficients suggest that while application of a primary ecosystem source may improve the model−measurement discrepancies for formic acid over forests described above, a direct source may be mechanistically inaccurate. Further, formic acid basal emissions of 4700 nmol m^{-2} h^{-1} are 7 times larger than the 30 μg m^{-2} h^{-1} basal emissions used in previous studies to estimate formic acid emissions from trees and shrubs in forest ecosystems.[6,12] Thus, direct plant emissions are unlikely the sole source of the organic acids.

We observe few downward fluxes, meaning that local dry deposition is insufficient to overwhelm the sources and control the atmospheric lifetimes of any of the organic acids.

The observed, net ecosystem organic acid flux is temperature-dependent, occurs only during the daytime, and persists throughout the seasons. Here, we evaluate four possible contributing sources of organic acids: primary emissions from (1) plants, (2) soils, and (3) ants, plus (4) secondary, in-canopy chemistry of other biogenic VOC emissions. We compare these sources to predicted dry deposition sinks and consider the organic acid flux budget at MEFO.

6.1. Plant Emissions. Plants emit C1−C7 alkanoic acids and are a plausible primary source of observed upward flux.

DOI: 10.1021/acsearthspacechem.9b00182
ACS Earth Space Chem. 2019, 3, 2017−2032

Plants produce formic acid by oxidizing glyoxylic acid, methanol, and formaldehyde and by reducing CO_2 to formate.[75,76] Biochemical production mechanisms of the other organic C_2−C_7 acids discussed herein are scarce. To the best of our knowledge, direct emissions of propionic, methacrylic, butyric, valeric, and heptanoic acids from plants may be presented here for the first time. This could also be evidence of very rapid secondary chemical formation of organic acids from biogenic precursors.

Correlations of temperature and vapor pressure deficit with organic acid fluxes are consistent with direct plant emissions as are the observed seasonal trends in organic acid fluxes. Plant metabolism, including the formic acid-forming processes of ethylene synthesis and methanol oxidation, slows during colder seasons due to reduced temperatures and available sunlight. Likewise, organic acid emissions decrease by an order of magnitude between warm (summer and fall) and cold (winter and spring) seasons.

However, measurements of organic acid emissions from plants suggest relatively small fluxes, at least an order of magnitude smaller than known oxidative precursors such as isoprene and monoterpenes.[34] MEGAN incorporates leaf cuvette and branch enclosure measurements into emission factors used to predict plant emissions for formic, acetic, and pyruvic acids.[73] Applying the MEGAN temperature parametrization to MEFO predicts a summer mid-day leaf-level formic acid flux of 170 nmol m^{-2} h^{-1} in comparison to the observed 3400 nmol m^{-2} h^{-1}.

We can further refine these estimates of primary biogenic emission using previous studies of pine tree emissions of formic acid. To the best of our knowledge, there are no previous measurements of C3−C7 organic acid emissions from plants, let alone pine trees. Villanueva-Fierro et al. measured a mass emission rate of 210 ng_{HCOOH} $g_{d.w.}^{-1}$ h^{-1} from ponderosa pine in Central New Mexico.[77] Kesselmeier et al. measured an average mass emission rate of 333 ng_{HCOOH} $g_{d.w.}^{-1}$ h^{-1} from Italian stone pine (*Pinus pinea* L).[78] Dense pine forests with LAIs on the order of 2.5−4.0 have pine needle biomass densities of 400−900 $g_{d.w.}$ m^{-2}, and we estimate 200 $g_{d.w.}$ m^{-2} pine needle density at MEFO (LAI = 1.14).[79] We estimate formic acid basal emission rates from ponderosa pine trees (E_f), mass emission rate (E_{needle}, ng $g_{d.w.}^{-1}$ h^{-1}) and the density of pine needles in a characteristic area of forest (ρ_{needle}, $g_{d.w.}$ m^{-2}) from

$$E_f = E_{needle}\rho_{needle} \quad (3)$$

Using the two published pine mass emission rates, we calculate a basal emission rate for formic acid of 910−1500 nmol m^{-2} h^{-1}, smaller than the 4700 nmol m^{-2} h^{-1} calculated from the ecosystem scale fluxes (Figure 3). Scaling these emission potentials to MEFO according to eq 2 using α = 0.09 and T_s = 303 K, we predict that direct plant emissions from ponderosa pine would account for mid-day fluxes of 630−1000 nmol m^{-2} h^{-1} of formic acid in summer and 140−220 nmol m^{-2} h^{-1} in winter. For comparison, Schobesberger et al. estimated a summer afternoon primary plant emission of formic acid at Hyytiala as ∼5 ppt_v m s^{-1} (∼500 nmol m^{-2} h^{-1}).[6] Besides predicted emissions for Italian stone pine, these literature-based estimates suggest that plant emissions account for little of the observed upward flux.

We compare these literature-based estimates of plant emissions to actual branch enclosure measurements. We enclosed a ponderosa pine branch ∼5 m a.g.l. in a Teflon bag and sampled the concentration gradient between ambient air outside versus inside the bag with the CIMS (see Section S2.1 for details). We observed very small primary plant emissions of organic acids with these in situ branch enclosures (Table 4). Scaling our observed leaf-level emission of formic acid to the forest leaf area results in a direct plant flux of formic acid of 94 nmol m^{-2} h^{-1}, just 2.5% of the summer daily maximum.

Table 4. Six Organic Acid Emissions from a Representative Ponderosa Pine[a]

	branch enclosure		soil chamber	
organic acid name	flux (nmol m^{-2} h^{-1})	% of measured flux	flux (nmol m^{-2} h^{-1})	% of measured flux
formic	94	2.5	1.1×10^{-2}	<1
propionic	26	41	6.9×10^{-4}	<1
methacrylic	2.6	18	-2.2×10^{-7}	<1
butyric	15	24	3.8×10^{-4}	<1
valeric	7.3	32	1.8×10^{-4}	<1
heptanoic	2.7	12	6.7×10^{-5}	<1

[a]Column 3 contains branch enclosure measurements of six organic acid emissions from a representative ponderosa pine. The percentage of average daily maximum fluxes represented by enclosure emissions follow in column 4. Averages of three soil chamber measurements of six volatile organic acid fluxes from soil and leaf litter and the percentage of the average daily maximum flux accounted for by the chamber average complete the table.

Our branch enclosure measurements suggest that while primary plant emissions are negligible for formic acid, they may be relatively important sources of the other organic acids during cold seasons. For example, during winter, plant emissions of butyric acid account for a large fraction (62%) of the measured flux + dry deposition. During spring, plant emissions overestimate (190%) the butyric acid flux budget.

6.2. Soil and Leaf Litter Emissions. Soils and leaf litter can be direct sources of multiple organic acids via microbial activity.[80,81] Microbes of the *Propionibacterium* genus synthesize propanoic acid from succinate or pyruvate intermediaries following glycolysis. Similarly, butyric acid is synthesized by glycolytically formed pyruvate oxidizing to Acetyl CoA; butyric acid can be further processed by fermentation. Mixed acid synthesis can produce formic, acetic, lactic, butyric, and succinic acids through alternate end-pathways to fermentation for many microbes. Ubiquitous methanotrophic bacteria synthesize formic acid from subsequent steps following the oxidation of methane prior to initiation of the serine cycle.

Sanhueza and Andreae measured daily average formic acid emissions of 0.14 nmol m^{-2} s^{-1} from dry, savannah soils in Venezuela.[82] On the basis of these measurements, Paulot et al. developed an exponential relationship between soil emissions of HCOOH (E_{soil}) and temperature[12]

$$E_{soil} = Ae^{((\beta \times T)-1)} \quad (4)$$

where A is the basal emission rate from soil (nmol m^{-2} h^{-1}), β is the temperature sensitivity, and T is soil temperature (°C). Paulot et al. found $A = 1.7 \times 10^{-3}$ nmol m^{-2} s^{-1} and β = 0.119 °C $^{-1}$.[12] The dry, deep, sandy loamy soils at MEFO have similar attributes to the savannah soils with neutral pH (6.1−7.8) and minimal organic content (1−4%).[50] Mielnik et al. measured soil formic acid fluxes of a similar magnitude (0.01−

DOI: 10.1021/acsearthspacechem.9b00182
ACS Earth Space Chem. 2019, 3, 2017−2032

0.15 nmol m^{-2} s^{-1}) from Colorado soils, including samples from MEFO collected in spring and summer 2018.[21] The Colorado soils showed larger basal emission rates but suppressed temperature dependences (A = 0.11 nmol m^{-2} s^{-1} and β = 0.028 °C^{-1}) relative to the tropical savannah soils. On the basis of these studies, we calculate that soil emits 49−300 nmol m^{-2} h^{-1} of formic acid during summer (1.3−8% of observed ecosystem flux) and 6.2−180 nmol m^{-2} h^{-1} during winter (2.9−84% of observed ecosystem flux). However, soil emissions depend on soil moisture, and these calculations do not consider that or potential emissions from leaf litter, nor do they provide soil emissions for organic acids other than formic or acetic acid.

We conducted in situ soil chamber experiments during fall 2016 to observationally constrain soil/forest floor emissions of formic and other organic acids. Gray et al. describe the soil chambers in detail.[83] We installed three chambers within the flux footprint into soil that was covered in needle detritus. Organic acid emissions from the chambers are consistently small, accounting for <1% of the observed fall fluxes (Table 4). Soils emit more formic acid than the other organic acids, consistent with a methanotrophic bacteria source. The observed formic acid emission is an order of magnitude smaller than the previous two studies, which we speculate is due to (i) the cooler ambient temperatures than those explored in laboratory experiments, (ii) potential organic acid uptake by the needle litter layer, and (iii) the very dry conditions during the soil chamber studies. MEFO experienced no precipitation for ∼4 weeks during the fall before soil chamber measurements were conducted, and the soil was likely much drier than previous lab or field experiments. Considering both the literature and in situ chamber constraints, soils are a small atmospheric source for any of the organic acids.

The persistent upward fluxes observed during winter and spring raise the question of snow as an organic acid source. A thick (>30 cm) layer of snow covered the forest floor at MEFO four times during SPiFFY, twice during winter, and twice during spring. Surprisingly, these events impacted neither the diel cycle, nor the magnitude of organic acid fluxes (Figure 4).

6.3. Ant Emissions. Formicine ants emit formic acid for defense and alarm signaling.[23] *Formica podzolica* is an abundant ant species at a nearby site in the forest (39.1° N, 105.0833° W).[84] We estimate ant emissions at Manitou by eq 5 following Graedel and Eisner[23]

$$F_{ants} = \frac{\rho_a m_a \psi}{\delta} \quad (5)$$

where F_{ants} is formic acid flux from *Formica* sp. ants, ρ_a is the estimated density of ants (100−600 ants m^{-2}), m_a is average ant mass (5 mg), φ is fraction of ant body mass present as volatilizable formic acid (0.02), and δ is the time scale for formic acid release (0.5 yr). Ant density is based upon two studies of *Formica* ant ecology in Colorado, which found colony densities between 15−115 mounds ha^{-1}.[85,86] Assuming 5×10^5 ants $mound^{-1}$, we estimate ant densities between 100−600 ants m^{-2}. We calculate that ants contribute 54−300 nmol m^{-2} h^{-1} of the formic acid flux in the summer, or 1−8% of the measured daily maximum formic acid flux. Ants hibernate in the colder seasons, and we assume they are negligible formic acid sources in winter and spring at Manitou. Ants and other fauna are not known sources of the other five organic acids.

6.4. In-Canopy Chemistry. Multigenerational oxidation of volatile organic compounds produces much of the known formic acid budget.[12,14,15] For example, monoterpenes with terminal alkenes, such as beta pinene and limonene, can be oxidized by O_3 to form stabilized Criegee intermediates (CH_2OO). The Criegee biradical can then react with readily available water vapor ($k = 1 \times 10^{-17}$ cm^3 $molec^{-1}$ s^{-1}) and generate formic acid. In fact, H_2O + different Criegee intermediates and HO_2 or RO_2 + a peroxyacyl radical constitute the primary formation reactions for alkanoic acids employed by the Master Chemical Mechanism via the Web site: http://mcm.leeds.ac.uk/MCM.[87,88]

Organic acid formation throughout a well-mixed boundary layer should not affect observed ecosystem-atmosphere fluxes unless there is a strong vertical gradient in production. However, in-canopy chemistry is a known phenomenon in which fast chemical reactions on the time scale of forest canopy residence times (<10 min) create vertical gradients in concentration below the sensor height and thus an observed turbulent flux. In-canopy chemistry is thought to cause enhanced deposition fluxes of O_3 and enhanced upward fluxes of NO_x, NO_y, and secondary organic aerosol.[89−92] Production reactions must be faster than the canopy air exchange rate below the sensor height to cause observed upward fluxes, requiring substantial emissions of very reactive precursors. However, ponderosa pine trees are strong emitters of monoterpenes and other VOCs.[39,93] Alwe et al. speculate that in-canopy chemistry is responsible for upward formic acid fluxes, providing correlations between formic acid and oxidized organic compounds as supporting evidence.[13] In-canopy ozonolysis and OH oxidation of biogenic VOC emissions are thus potential ecosystem sources of organic acids.

Several lines of evidence point to the possible role of in-canopy chemistry in the observed MEFO ecosystem source of organic acids. The temperature-dependence of observed organic acid emissions is similar to that of biogenic VOC precursors, and monoterpenes in particular. Kaser et al. (2013) found temperature-dependent fit parameters for eq 2 of E_f = 0.50 mg m^{-2} h^{-1} and β = 0.12.[39] Using these parameters and ambient temperatures measured during SPiFFY, we estimate monoterpene emissions of 0−0.49 mg m^{-2} h^{-1}, which accounts for 0−36 μmolC m^{-2} h^{-1} of organic carbon atoms, compared to the 0−3.8 μmolC m^{-2} h^{-1} observed emission for formic

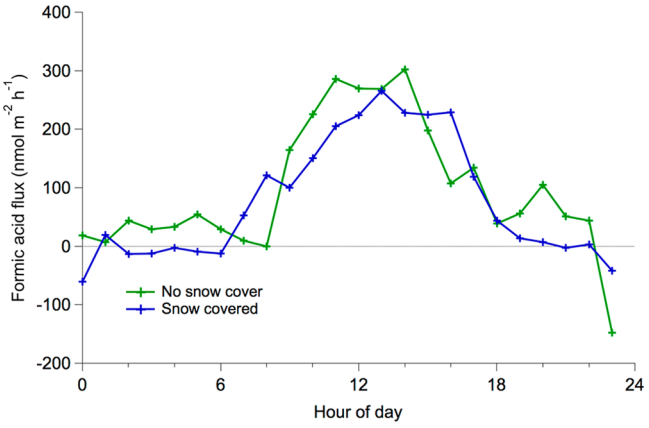

Figure 4. Diel averaged formic acid fluxes from February 25, 2016 (blue) and February 17, 2016 (green) are not substantively different in magnitude or trend with snow-covered ground (>30 cm) or bare ground in the same season and at afternoon maximum temperatures of 9.4 and 13 °C, respectively.

DOI: 10.1021/acsearthspacechem.9b00182
ACS Earth Space Chem. 2019, 3, 2017−2032

acid. There is little correlation between formic acid flux and either O_3 or PPFD, which would influence available O_3 or OH, but the oxidant might not be the limiting reactant in the organic acid production. Thus, a clear correlation is not necessarily expected.

For in-canopy chemistry to produce an observed upward organic acid flux, several requirements must be met. First, in-canopy production must outcompete in-canopy deposition. Second, the forest must have enough oxidant in the canopy and emit enough fast-reacting VOCs so as to outcompete production of organic acids above the sensor height on the time scale of canopy−atmosphere exchange, thereby producing a vertical gradient in organic acids. Ponderosa pines at Manitou emit 2-methyl-3-buten-2-ol (MBO) (50.2% of total BVOC emissions) and monoterpenes (33.5%), which account for ∼62% of the OH reactivity at the site.[94] NO^+ CIMS measured isoprene concentrations of ∼200 ppt_v at MEFO.[95]

Multigenerational reactions of O_3 and OH with terpenes produce formic acid. Formic acid yields from MBO are 6−8% with OH and 3% with O_3.[96] Formic acid yields from monoterpenes are 4−11% with OH and 7% with O_3.[97,98] We calculate the chemical production by

$$\mathrm{Flux}_{\mathrm{HCOOH}} = \mathrm{Flux}_{\mathrm{precursor}} \times k_{\mathrm{oxidant}} \times C_{\mathrm{oxidant}} \times \tau \times Y \quad (6)$$

where $\mathrm{Flux}_{\mathrm{HCOOH}}$ is the predicted chemical production flux of formic acid, $\mathrm{Flux}_{\mathrm{precursor}}$ is the average daily maximum flux of MBO from Kaser et al. or the average daily maximum flux of monoterpenes calculated from the E_f and β parameters of Kaser et al. given observed meteorological conditions and eq 2,[39] k_{oxidant} is the rate constant of the corresponding precursor with OH or O_3, C_{oxidant} is the concentration of OH or O_3, τ is the canopy residence time, and Y is the appropriate molar yield. The canopy residence time is estimated from the findings of Martens et al., who report residence times for radon, a transport tracer for CO_2 exchange between the atmosphere and a forest canopy.[99] Given summertime daily maximum fluxes of 0.31 mg m^{-2} h^{-1} for monoterpenes and 2.2 mg m^{-2} h^{-1} for MBO, an estimated canopy OH concentration of 1×10^6 molecules cm^{-3}, a canopy residence time of 10 min, and rate constants (k_{OH}) of 1×10^{-10} and 3.9×10^{-11} cm^3 $molec^{-1}$ s^{-1} for monoterpenes and MBO, respectively, we predict 45 and 42 nmol m^{-2} h^{-1} formic acid from in-canopy OH oxidation of monoterpenes and MBO, respectively. In-canopy OH oxidation calculated according to eq 6 accounts for at most 1% (monoterpenes) and 1% (MBO) of the average midday measured formic acid flux of 3500 nmol m^{-2} h^{-1}. Using the same biogenic hydrocarbon emissions, a measured average daily maximum O_3 concentration of 107×10^{10} molecules cm^{-3} (∼60 ppb_v), and k_{ozone} values of 3.9×10^{-15} and 8.6×10^{-18} cm^3 $molec^{-1}$ s^{-1} for monoterpenes and MBO, respectively, we calculate formic acid fluxes of 1190 and 2.5 nmol m^{-2} h^{-1} following eq 6. These afternoon maximum production fluxes account for 35% and <1% of the net formic acid flux from monoterpene and MBO ozonolysis, respectively. We note that formic acid yields vary with oxidant exposure and in-canopy chemistry must occur within 10 min to contribute to an observed upward flux, so these yields used in these calculations represent upper estimates.[28]

These back-of-the-envelope calculations thus imply that in-canopy oxidation of reactive biogenic VOCs, and ozonolysis of monoterpenes in particular, may be substantial components of the observed organic acid flux. Ozone changes little across the seasons (Table 2), but the temperature decreases substantially in the winter and spring meaning that the temperature-dependent monoterpene and MBO emissions will also decrease. Thus, we estimate that in-canopy chemistry will cause 120 nmol m^{-2} h^{-1} of formic acid flux in the winter or 59% of the observed flux.

OH oxidation of monoterpenes produces 0.002−0.06% molar yields of methacrylic and butyric acids, which would result in upward fluxes of 3.0 and 2.5 nmol m^{-2} h^{-1} of methacrylic and butyric acids, respectively, in summer.[28] Here, we calculate chemical production with a weighted average assuming 33.3% of total monoterpenes each represented by alpha pinene, beta pinene, and limonene. A more detailed canopy chemistry model may be able to better constrain some of the potential sources that we identify here. For example, peroxy radicals are present at MEFO in mixing ratios as high as 180 ppt_v and can react with other RO_2 or HO_2 radicals to produce gaseous organic acids.[100]

6.5. Flux Budget. We combine the observational and literature-derived constraints on each of the organic acid sources and sinks to create a flux budget. We focus on mid-day fluxes, when the observed ecosystem organic acid sources are at their largest. We calculate dry deposition with a resistance model, including canopy resistance improvements from Nguyen et al.[40,101] A detailed description of the resistance model is provided in Section S3. The observed flux is the net result of sources minus sinks, so we calculate an organic acid source term as the sum of observed flux plus calculated dry deposition.

We compare the "bottom-up" formic acid source (i.e., sum of individually calculated components discussed above) to the "top-down" source determined as the sum of observed flux + calculated dry deposition. We see excellent agreement for formic acid sources at night, but strong discrepancies in the day (Figure 5). Chemical production, specifically rapid ozonolysis of monoterpenes in the canopy, is predicted to be the single largest source of formic acid. Thus, we find a missing/underestimated formic acid source and potentially an overestimated formic acid sink. With the exception of

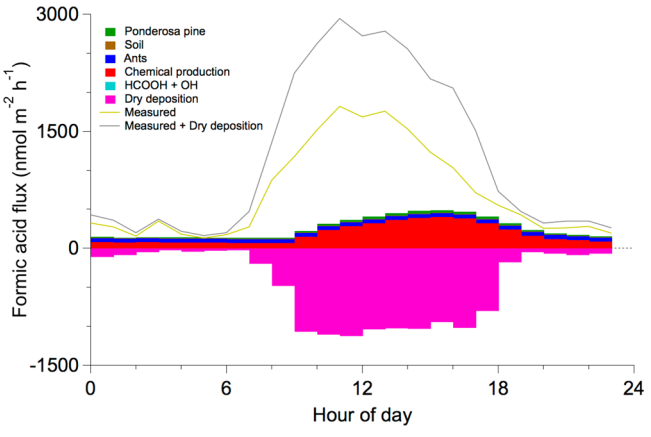

Figure 5. Diel formic acid flux budget for SPiFFY fall campaign. Budget totals represent the sum of all sources and sinks, measured where available and modeled using upper-bound estimates. The budget total accounts for approximately one-third of the measured daytime flux. The budget total poorly recreates the substantial difference between day and nighttime fluxes seen in the measured fluxes.

DOI: 10.1021/acsearthspacechem.9b00182
ACS Earth Space Chem. 2019, 3, 2017−2032

methacrylic acid, canopy-level fluxes are far larger in warm seasons than cold seasons (Figure 6). During winter, summer,

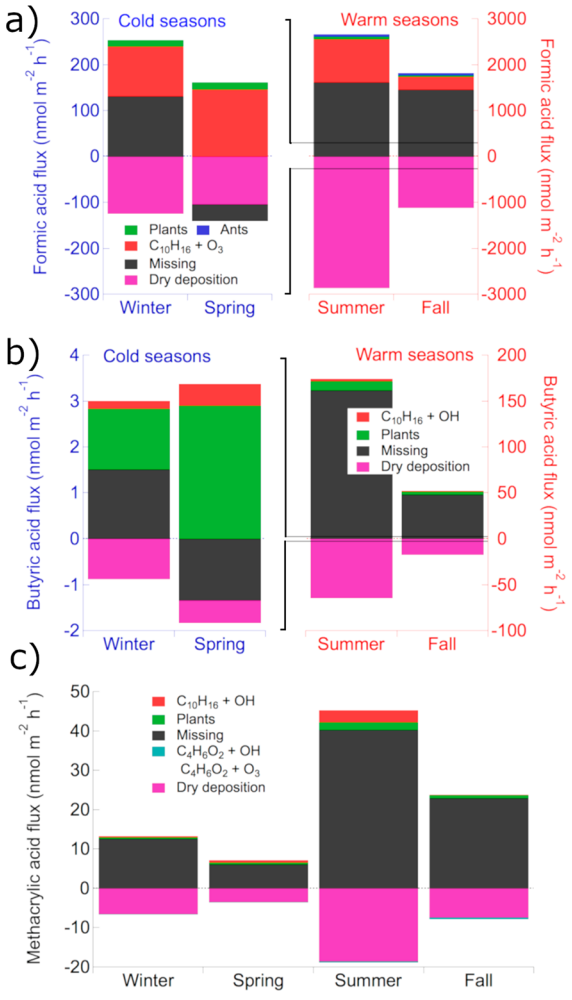

Figure 6. Seasonal budgets of (a) formic, (b) butyric, and (c) methacrylic acid fluxes (nmol m^{-2} h^{-1}) increase in magnitude substantially during summer and fall. Winter and spring (cold seasons, blue) are separated from summer and fall (warm seasons, red) for butyric and formic acid budgets. Brackets relate the scale of cold season axes to the warm seasons. Budget values are chosen according to the hour of day at which the sum of the measured flux and dry deposition is maximized during each season.

and fall, sizable upward fluxes of formic acid are missing in the budgets. During spring, we overestimate sources (or underestimate sinks). This is one season with substantial snow cover, which we speculate may affect dry deposition, although this observation may also be the result of uncertainties around the relatively small observed flux. Secondary chemical production is the most important predicted source of formic acid across all seasons. In contrast, neither methacrylic nor butyric acid sources are controlled by chemical production. Most of these acids' budgets are controlled by missing sources except for during cold seasons when plant emissions become an important source for butyric acid. Like formic acid, butyric acid shows a missing sink or overestimated source during spring.

There are three ways to improve the comparison of modeled versus observed organic acid fluxes: (1) ecosystem source component(s) may be missing or underestimated, (2) missing and/or underestimated source(s) in combination with overestimated deposition, or (3) there may be a missing sink that is greatly enhanced above the sensor height relative to below. Missing sources could include:

- In-canopy chemistry of sesquiterpenes, which are emitted from ponderosa pines[102] and react rapidly with O_3,[103] though their organic acid yields are unknown. Ponderosa pines also emit other terpenoids, including methyl chavicol, which are also likely oxidized to form organic acids.[104] We also note that different monoterpene isomers produce different amounts and distributions of organic acids.[28]
- Reactions of O_3 with ecosystem sources (e.g., epicuticular waxes, cellulose, or lignin on branch surfaces, exposed pine resins, and/or organic matter on soil surfaces); although ozonolysis of plant biomass has been noted to produce formic acid,[105] the lack of correlation between ozone and upward organic acid fluxes makes this unlikely.
- Dew or water layers on ecosystem surfaces may act as an organic acid reservoir, absorbing organic acids at night and then evaporating and releasing them during the day. Studies of ammonia have found that surface moisture can account for a sizable fraction of morning emissions.[106] We would expect a morning increase in organic acid emissions from the forest, which is seen in both the concentration and flux data (Figure 2).
- Direct emissions from biogenic sources not constrained with measurements in this study, such as herbaceous plants on the forest floor, tree trunks, fallen branches, and pine resins.[3,107−109]

Alternately, the top-down approach may overestimate the organic acid sinks. Removal of organic acid by OH radicals or O_3 are negligible relative to dry deposition and cannot account for the model-measurement discrepancy. However, our understanding of dry deposition of oxygenated VOCs is limited, and a more likely source of uncertainty. Although not included in our dry deposition resistance model, volatile organic acids can be lost to particles through gas-particle partitioning and reactions at particle surfaces. However, previous studies suggest that aqueous-phase partitioning does not contribute significantly to ambient organic acid mixing ratios with calculated organic acid losses to particles of 6.1×10^{-11} to 2.4×10^{-8} ppb_v.[44] MEFO in the summer and fall is typically arid and is thus likely to have limited water surfaces to which the water-soluble organic acids in this study could be lost. Gases may not be removed to forest surfaces with the same efficiency as wetter environments. Further investigation of dry deposition mechanisms for oxidized organic species is essential for understanding the role of the terrestrial biosphere in regulating organic acid concentrations in the atmosphere.

Organic acid loss processes that are far faster above the sensor height than below would create a decreasing vertical gradient throughout the boundary layer and an apparent upward flux. That is, the flux discrepancy could be driven by an atmospheric loss process rather than an ecosystem source. Possible organic acid loss processes above the sensor height include entrainment of clean air from the free troposphere, removal by dissolution in cloud droplets, or more rapid photolysis or oxidation higher up in the boundary layer. One possible chemical loss for organic acids that are unexplored in the atmospheric chemistry literature is the esterification reaction of carboxylic acids with alcohols, such as methanol. An atmospheric loss process that is enhanced with altitude would also explain the diel cycles in organic acid mixing ratio:

DOI: 10.1021/acsearthspacechem.9b00182
ACS Earth Space Chem. 2019, 3, 2017−2032

the afternoon drop-off in organic acid mixing ratio requires a rapid loss process. Although dry deposition is typically invoked to explain diel cycles from ground observations of nitric acid (HNO_3), the organic acid flux measurements during SPiFFY are upward throughout the day. Thus, ecosystem sources consistently outcompete dry deposition. A removal process higher in the atmosphere would help explain both the observed upward flux and the short lifetime implied by the mixing ratio diel cycle. However, we note that Mattila et al. did not observe any evidence for strong sinks higher in the boundary layer from vertical profiles of organic acids in the Front Range of Colorado and that those vertical profile observations were more consistent with surface-level sources such as ozonolysis of surface organic matter, such as vegetation, soils, or organic films.[21]

7. CONCLUSIONS

We observe a consistent ecosystem source of organic acids throughout all four seasons at this semiarid ponderosa pine forest site. Organic acid fluxes from the forest increase exponentially with temperature similar to monoterpene fluxes. MEFO is clearly a net source of organic acids to the atmosphere throughout the year although the fluxes are largest in the warmer summer and fall months. The observed emission fluxes can be partially accounted for by known and observed primary and secondary sources; however, the relative importance of these sources varies for each organic acid. Soils and pine trees are predicted to be negligible sources of formic acid relative to in-canopy chemical production but may be more important for other organic acids, particularly in colder seasons when emissions of reactive terpenoids and subsequent in-canopy chemistry are small. Formic acid may be a valuable tracer for the chemical flux of ozone. Assuming a daytime ozone flux of ∼−40 μmol m^{-2} h^{-1}, a production flux of 1190 nmol m^{-2} h^{-1} suggests that ∼3% of the ozone flux signal could be attributed to formic acid production from ozonolysis reactions with monoterpenes. A missing source (or overestimated sink below the canopy height or underestimated sink above) remains not only for formic acid but also butyric and methacrylic acids. Potential organic acid sources include in-canopy gas or surface oxidation chemistry or interaction with water layers on ecosystem surfaces. We may also be overestimating dry deposition in the arid Colorado environment and/or ignoring organic acid sinks higher in the boundary layer. Our observations highlight the uncertainties in understanding the sources and sinks of even the simplest oxidized VOCs in the atmosphere and point to a need for a deeper mechanistic understanding of dry deposition of organic gases, emission of larger and multifunctional terpenoids, and rapid oxidation chemistry occurring in forest canopies. Removal processes for organic acids remain puzzling, as the diel concentration profiles suggest a strong afternoon sink, but our flux observations demonstrate that dry deposition is insufficient to outcompete the ecosystem sources.

ASSOCIATED CONTENT

Supporting Information

The Supporting Information is available free of charge on the ACS Publications website at DOI: 10.1021/acsearthspacechem.9b00182.

CIMS calibrations, supporting measurements, and resistance modeling (PDF)

AUTHOR INFORMATION

Corresponding Author

*E-mail: Delphine.Farmer@colostate.edu.

ORCID

S. Ryan Fulgham: 0000-0002-3930-9131
Michael Link: 0000-0002-1841-2455
Delphine K. Farmer: 0000-0002-6470-9970

Present Address

[‖]Waters Corporation, 34 Maple St. Milford, MA 01757,U.S.A.

Author Contributions

P.B. designed and built the field deployment system for CIMS measurements with assistance from R.F. P.B. and M.L. assisted R.F. with field deployments. J.O. and I.P. deployed supplemental measurement systems for trace gases. R.F. performed all analyses and drafted the figures with input from D.F. R.F. wrote the paper with suggestions from all coauthors, particularly D.F.

Funding

The research was funded by NOAA (Grant NA14OAR4310141) however the publication was neither reviewed nor any views endorsed by the organization.

Notes

The authors declare no competing financial interest.

ACKNOWLEDGMENTS

We thank Steven Alton (U.S. Forest Service) for logistical support in the field. We also thank Dr. Noah Fierer for use of his soil chambers and Dr. Robert Rhew for use of his branch enclosure system. We thank Dr. Julian Deventer for helpful conversations and Dr. Boris Kondratieff for assistance estimating ant population densities in Colorado.

REFERENCES

(1) Chebbi, A.; Carlier, P. Carboxylic Acids in the Troposphere, Occurrence, Sources, and Sinks: A Review. *Atmos. Environ.* **1996**, *30* (24), 4233−4249.

(2) Hellén, H.; Schallhart, S.; Praplan, A. P.; Petäjä, T.; Hakola, H. Using in Situ GC-MS for Analysis of C2−C7 Volatile Organic Acids in Ambient Air of a Boreal Forest Site. *Atmos. Meas. Tech.* **2017**, *10* (1), 281−289.

(3) Khare, P.; Kumar, N.; Kumari, K. M.; Srivastava, S. S. Atmospheric Formic and Acetic Acids: An Overview. *Rev. Geophys.* **1999**, *37* (2), 227−248.

(4) Liggio, J.; Moussa, S. G.; Wentzell, J.; Darlington, A.; Liu, P.; Leithead, A.; Hayden, K.; O'Brien, J.; Mittermeier, R. L.; Staebler, R.; et al. Understanding the Primary Emissions and Secondary Formation of Gaseous Organic Acids in the Oil Sands Region of Alberta, Canada. *Atmos. Chem. Phys.* **2017**, *17* (13), 8411−8427.

(5) Mellouki, A.; Wallington, T. J.; Chen, J. Atmospheric Chemistry of Oxygenated Volatile Organic Compounds: Impacts on Air Quality and Climate. *Chem. Rev.* **2015**, *115* (10), 3984−4014.

(6) Schobesberger, S.; Lopez-Hilfiker, F. D.; Taipale, D.; Millet, D. B.; D'Ambro, E. L.; Rantala, P.; Mammarella, I.; Zhou, P.; Wolfe, G. M.; Lee, B. H. High Upward Fluxes of Formic Acid from a Boreal Forest Canopy. *Geophys. Res. Lett.* **2016**, 2016GL069599.

(7) Vogel, A. L.; Äijälä, M.; Brüggemann, M.; Ehn, M.; Junninen, H.; Petäjä, T.; Worsnop, D. R.; Kulmala, M.; Williams, J.; Hoffmann, T. Online Atmospheric Pressure Chemical Ionization Ion Trap Mass Spectrometry (APCI-IT-MSn) for Measuring Organic Acids in Concentrated Bulk Aerosol − a Laboratory and Field Study. *Atmos. Meas. Tech.* **2013**, *6* (2), 431−443.

(8) Yatavelli, R. L. N.; Stark, H.; Thompson, S. L.; Kimmel, J. R.; Cubison, M. J.; Day, D. A.; Campuzano-Jost, P.; Palm, B. B.; Hodzic, A.; Thornton, J. A.; et al. Semicontinuous Measurements of Gas−

DOI: 10.1021/acsearthspacechem.9b00182
ACS Earth Space Chem. 2019, 3, 2017−2032

Particle Partitioning of Organic Acids in a Ponderosa Pine Forest Using a MOVI-HRToF-CIMS. *Atmos. Chem. Phys.* **2014**, *14* (3), 1527−1546.
(9) Davidson, C. I.; Phalen, R. F.; Solomon, P. A. Airborne Particulate Matter and Human Health: A Review. *Aerosol Sci. Technol.* **2005**, *39* (8), 737−749.
(10) IPCC, 2013. Contribution of Working Group I to the Fifth Assessment Report of the Intergovernmental Panel on Climate Change. In *Climate Change 2013: The Physical Science Basis*; Stocker, T. F.; Qin, D.; Plattner, G.-K.; Tignor, M.; Allen, S. K.; Boschung, J.; Nauels, A.; Xia, Y.; Bex, V.; Midgley, P. M., eds. Cambridge University Press: Cambridge, U.K., New York, 1535 pp, DOI: 10.1017/CBO9781107415324.
(11) Jacob, D. J. Chemistry of OH in Remote Clouds and Its Role in the Production of Formic Acid and Peroxymonosulfate. *J. Geophys. Res.* **1986**, *91* (D9), 9807−9826.
(12) Paulot, F.; Wunch, D.; Crounse, J. D.; Toon, G. C.; Millet, D. B.; DeCarlo, P. F.; Vigouroux, C.; Deutscher, N. M.; González Abad, G.; Notholt, J.; et al. Importance of Secondary Sources in the Atmospheric Budgets of Formic and Acetic Acids. *Atmos. Chem. Phys.* **2011**, *11* (5), 1989−2013.
(13) Alwe, H. D.; Millet, D. B.; Chen, X.; Raff, J. D.; Payne, Z. C.; Fledderman, K. Oxidation of Volatile Organic Compounds as the Major Source of Formic Acid in a Mixed Forest Canopy. *Geophys. Res. Lett.* **2019**, *46* (5), 2940−2948.
(14) Millet, D. B.; Baasandorj, M.; Farmer, D. K.; Thornton, J. A.; Baumann, K.; Brophy, P.; Chaliyakunnel, S.; de Gouw, J. A.; Graus, M.; Hu, L.; et al. A Large and Ubiquitous Source of Atmospheric Formic Acid. *Atmos. Chem. Phys.* **2015**, *15* (11), 6283−6304.
(15) Stavrakou, T.; Müller, J.-F.; Peeters, J.; Razavi, A.; Clarisse, L.; Clerbaux, C.; Coheur, P.-F.; Hurtmans, D.; De Mazière, M.; Vigouroux, C.; et al. Satellite Evidence for a Large Source of Formic Acid from Boreal and Tropical Forests. *Nat. Geosci.* **2012**, *5* (1), 26−30.
(16) Hellén, H.; Schallhart, S.; Praplan, A. P.; Petäjä, T.; Hakola, H. Using in Situ GC-MS for Analysis of C2-C7 Volatile Organic Acids in Ambient Air of a Boreal Forest Site. *Atmos. Meas. Tech.* **2017**, *10*, 281−289.
(17) Andreae, M. O.; Talbot, R. W.; Andreae, T. W.; Harriss, R. C. Formic and Acetic Acid over the Central Amazon Region, Brazil: 1. Dry Season. *J. Geophys. Res.* **1988**, *93* (D2), 1616−1624.
(18) Keene, W. C.; Galloway, J. N. Organic Acidity in Precipitation of North America. *Atmos. Environ.* **1984**, *18* (11), 2491−2497.
(19) Kesselmeier, J. Exchange of Short-Chain Oxygenated Volatile Organic Compounds (VOCs) between Plants and the Atmosphere: A Compilation of Field and Laboratory Studies. *J. Atmos. Chem.* **2001**, *39* (3), 219−233.
(20) Kesselmeier, J.; Bode, K.; Gerlach, C.; Jork, E.-M. Exchange of Atmospheric Formic and Acetic Acids with Trees and Crop Plants under Controlled Chamber and Purified Air Conditions. *Atmos. Environ.* **1998**, *32* (10), 1765−1775.
(21) Mielnik, A.; Link, M.; Mattila, J.; Fulgham, S. R.; Farmer, D. K. Emission of Formic and Acetic Acids from Two Colorado Soils. *Environ. Sci. Process. Impacts* **2018**, *20*, 1537−1545.
(22) Peñuelas, J.; Asensio, D.; Tholl, D.; Wenke, K.; Rosenkranz, M.; Piechulla, B.; Schnitzler, J. p. Biogenic Volatile Emissions from the Soil. *Plant, Cell Environ.* **2014**, *37* (8), 1866−1891.
(23) Graedel, T. E.; Eisner, T. Atmospheric Formic Acid from Formicine Ants: A Preliminary Assessment. *Tellus, Ser. B* **1988**, *40B* (5), 335−339.
(24) Calvert, J. G.; Su, F.; Bottenheim, J. W.; Strausz, O. P. Mechanism of the Homogeneous Oxidation of Sulfur Dioxide in the Troposphere. *Atmos. Environ.* **1978**, *12* (1), 197−226.
(25) Horie, O.; Neeb, P.; Limbach, S.; Moortgat, G. K. Formation of Formic Acid and Organic Peroxides in the Ozonolysis of Ethene with Added Water Vapour. *Geophys. Res. Lett.* **1994**, *21* (14), 1523−1526.
(26) Calvert, J. G.; Madronich, S. Theoretical Study of the Initial Products of the Atmospheric Oxidation of Hydrocarbons. *J. Geophys. Res.* **1987**, *92* (D2), 2211−2220.
(27) Chameides, W. L.; Davis, D. D. Aqueous-Phase Source of Formic Acid in Clouds. *Nature* **1983**, *304* (5925), 427−429.
(28) Friedman, B.; Farmer, D. K. SOA and Gas Phase Organic Acid Yields from the Sequential Photooxidation of Seven Monoterpenes. *Atmos. Environ.* **2018**, *187*, 335−345.
(29) Chattopadhyay, A.; Chatterjee, P.; Chakraborty, T. Photo-oxidation of Acetone to Formic Acid in Synthetic Air and Its Atmospheric Implication. *J. Phys. Chem. A* **2015**, *119* (29), 8146−8155.
(30) Crutzen, P. J.; Andreae, M. O. Biomass Burning in the Tropics: Impact on Atmospheric Chemistry and Biogeochemical Cycles. *Science* **1990**, *250* (4988), 1669−1678.
(31) Goldstein, A. H.; Galbally, I. E. Known and Unexplored Organic Constituents in the Earth's Atmosphere. *Environ. Sci. Technol.* **2007**, *41* (5), 1514−1521.
(32) Dawson, G. A.; Farmer, J. C. Soluble Atmospheric Trace Gases in the Southwestern United States: 2. Organic Species HCHO, HCOOH, CH3COOH. *J. Geophys. Res.* **1988**, *93* (D5), 5200−5206.
(33) Wine, P. H.; Astalos, R. J.; Mauldin, R. L. Kinetic and Mechanistic Study of the Hydroxyl + Formic Acid Reaction. *J. Phys. Chem.* **1985**, *89* (12), 2620−2624.
(34) Graedel, T. E. *Chemical Compounds in the Atmosphere*; Academic Press, 1978.
(35) Rosado-Reyes, C. M.; Francisco, J. S. Atmospheric Oxidation Pathways of Acetic Acid. *J. Phys. Chem. A* **2006**, *110* (13), 4419−4433.
(36) Graedel, T. E.; Weschler, C. J. Chemistry within Aqueous Atmospheric Aerosols and Raindrops. *Rev. Geophys.* **1981**, *19* (4), 505−539.
(37) Jardine, K.; Yañez Serrano, A.; Arneth, A.; Abrell, L.; Jardine, A.; Artaxo, P.; Alves, E.; Kesselmeier, J.; Taylor, T.; Saleska, S.; et al. Ecosystem-Scale Compensation Points of Formic and Acetic Acid in the Central Amazon. *Biogeosciences* **2011**, *8* (12), 3709−3720.
(38) Juráň, S.; Pallozzi, E.; Guidolotti, G.; Fares, S.; Šigut, L.; Calfapietra, C.; Alivernini, A.; Savi, F.; Večeřová, K.; Křůmal, K.; et al. Fluxes of Biogenic Volatile Organic Compounds above Temperate Norway Spruce Forest of the Czech Republic. *Agric. For. Meteorol.* **2017**, *232*, 500−513.
(39) Kaser, L.; Karl, T.; Guenther, A.; Graus, M.; Schnitzhofer, R.; Turnipseed, A.; Fischer, L.; Harley, P.; Madronich, M.; Gochis, D.; et al. Undisturbed and Disturbed above Canopy Ponderosa Pine Emissions: PTR-TOF-MS Measurements and MEGAN 2.1 Model Results. *Atmos. Chem. Phys.* **2013**, *13* (23), 11935−11947.
(40) Nguyen, T. B.; Crounse, J. D.; Teng, A. P.; St. Clair, J. M.; Paulot, F.; Wolfe, G. M.; Wennberg, P. O. Rapid Deposition of Oxidized Biogenic Compounds to a Temperate Forest. *Proc. Natl. Acad. Sci. U. S. A.* **2015**, *112* (5), E392−E401.
(41) Park, J.-H.; Goldstein, A. H.; Timkovsky, J.; Fares, S.; Weber, R.; Karlik, J.; Holzinger, R. Active Atmosphere-Ecosystem Exchange of the Vast Majority of Detected Volatile Organic Compounds. *Science* **2013**, *341* (6146), 643−647.
(42) Schallhart, S.; Rantala, P.; Kajos, M. K.; Aalto, J.; Mammarella, I.; Ruuskanen, T. M.; Kulmala, M. Temporal Variation of VOC Fluxes Measured with PTR-TOF above a Boreal Forest. *Atmos. Chem. Phys.* **2018**, *18* (2), 815−832.
(43) Shaw, W. J.; Spicer, C. W.; Kenny, D. V. Eddy Correlation Fluxes of Trace Gases Using a Tandem Mass Spectrometer. *Atmos. Environ.* **1998**, *32* (17), 2887−2898.
(44) Mattila, J. M.; Brophy, P.; Kirkland, J.; Hall, S.; Ullmann, K.; Fischer, E. V.; Brown, S.; McDuffie, E.; Tevlin, A.; Farmer, D. K. Tropospheric Sources and Sinks of Gas-Phase Acids in the Colorado Front Range. *Atmos. Chem. Phys.* **2018**, *18* (16), 12315−12327.
(45) Friedman, B.; Link, M. F.; Fulgham, S. R.; Brophy, P.; Galang, A.; Brune, W. H.; Jathar, S. H.; Farmer, D. K. Primary and Secondary Sources of Gas-Phase Organic Acids from Diesel Exhaust. *Environ. Sci. Technol.* **2017**, *51* (18), 10872−10880.
(46) Kawamura, K..; Ng, L. L..; Kaplan, I. R. Determination of Organic Acids (C1-C10) in the Atmosphere, Motor Exhausts, and Engine Oils. *Environ. Sci. Technol.* **1985**, *19* (11), 1082−1086.

DOI: 10.1021/acsearthspacechem.9b00182
ACS Earth Space Chem. 2019, 3, 2017−2032

(47) Mungall, E. L.; Abbatt, J. P. D.; Wentzell, J. J. B.; Lee, A. K. Y.; Thomas, J. L.; Blais, M.; Gosselin, M.; Miller, L. A.; Papakyriakou, T.; Willis, M. D.; et al. Microlayer Source of Oxygenated Volatile Organic Compounds in the Summertime Marine Arctic Boundary Layer. *Proc. Natl. Acad. Sci. U. S. A.* **2017**, *114* (24), 6203−6208.
(48) Mungall, E. L.; Abbatt, J. P. D.; Wentzell, J. J. B.; Wentworth, G. R.; Murphy, J. G.; Kunkel, D.; Gute, E.; Tarasick, D. W.; Sharma, S.; Cox, C. J.; et al. High Gas-Phase Mixing Ratios of Formic and Acetic Acid in the High Arctic. *Atmos. Chem. Phys.* **2018**, *18* (14), 10237−10254.
(49) Veres, P. R.; Roberts, J. M.; Cochran, A. K.; Gilman, J. B.; Kuster, W. C.; Holloway, J. S.; Graus, M.; Flynn, J.; Lefer, B.; Warneke, C.; et al. Evidence of Rapid Production of Organic Acids in an Urban Air Mass. *Geophys. Res. Lett.* **2011**, *38* (17), L17807.
(50) Ortega, J.; Turnipseed, A.; Guenther, A. B.; Karl, T. G.; Day, D. A.; Gochis, D.; Huffman, J. A.; Prenni, A. J.; Levin, E. J. T.; Kreidenweis, S. M.; et al. Overview of the Manitou Experimental Forest Observatory: Site Description and Selected Science Results from 2008 to 2013. *Atmos. Chem. Phys.* **2014**, *14* (12), 6345−6367.
(51) Asherin, L. A. *Manitou Experimental Forest Hourly Meteorology Data*, 2nd ed.; Forest Service Research Data Archive: Fort Collins, CO, 2016.
(52) Brophy, P.; Farmer, D. K. A Switchable Reagent Ion High Resolution Time-of-Flight Chemical Ionization Mass Spectrometer for Real-Time Measurement of Gas Phase Oxidized Species: Characterization from the 2013 Southern Oxidant and Aerosol Study. *Atmos. Meas. Tech.* **2015**, *8* (7), 2945−2959.
(53) Brophy, P.; Farmer, D. K. Clustering, Methodology, and Mechanistic Insights into Acetate Chemical Ionization Using High-Resolution Time-of-Flight Mass Spectrometry. *Atmos. Meas. Tech.* **2016**, *9* (8), 3969−3986.
(54) Roberts, J. M.; Veres, P.; Warneke, C.; Neuman, J. A.; Washenfelder, R. A.; Brown, S. S.; Baasandorj, M.; Burkholder, J. B.; Burling, I. R.; Johnson, T. J.; et al. Measurement of HONO, HNCO, and Other Inorganic Acids by Negative-Ion Proton-Transfer Chemical-Ionization Mass Spectrometry (NI-PT-CIMS): Application to Biomass Burning Emissions. *Atmos. Meas. Tech.* **2010**, *3* (4), 981.
(55) Veres, P.; Roberts, J. M.; Warneke, C.; Welsh-Bon, D.; Zahniser, M.; Herndon, S.; Fall, R.; de Gouw, J. Development of Negative-Ion Proton-Transfer Chemical-Ionization Mass Spectrometry (NI-PT-CIMS) for the Measurement of Gas-Phase Organic Acids in the Atmosphere. *Int. J. Mass Spectrom.* **2008**, *274* (1−3), 48−55.
(56) Pagonis, D.; Krechmer, J. E.; de Gouw, J.; Jimenez, J. L.; Ziemann, P. J. Effects of Gas−Wall Partitioning in Teflon Tubing and Instrumentation on Time-Resolved Measurements of Gas-Phase Organic Compounds. *Atmos. Meas. Tech.* **2017**, *10* (12), 4687−4696.
(57) Gill Instruments Ltd. *Software Bug Affecting 'w' Wind Component of the WindMaster Family*; technical key note KN1509v3*; 2016.
(58) Mauder, M.; Cuntz, M.; Drüe, C.; Graf, A.; Rebmann, C.; Schmid, H. P.; Schmidt, M.; Steinbrecher, R. A Strategy for Quality and Uncertainty Assessment of Long-Term Eddy-Covariance Measurements. *Agric. For. Meteorol.* **2013**, *169*, 122−135.
(59) Tanner, C. B.; Thurtell, G. W. Anemoclinometer Measurements of Reynolds Stress and Heat Transport in the Atmospheric Surface Layer. Wisconsin Univ-Madison Dept of Soil Science, Research and Development Technical Report ECOM 66-G22-F to the U.S. Army Electronics Command, 1969.
(60) Baldocchi, D. D. Assessing the Eddy Covariance Technique for Evaluating Carbon Dioxide Exchange Rates of Ecosystems: Past, Present and Future. *Glob. Change Biol.* **2003**, *9* (4), 479−492.
(61) Webb, E. K.; Pearman, G. I.; Leuning, R. Correction of Flux Measurements for Density Effects Due to Heat and Water Vapour Transfer. *Q. J. R. Meteorol. Soc.* **1980**, *106* (447), 85−100.
(62) Papale, D.; Reichstein, M.; Aubinet, M.; Canfora, E.; Bernhofer, C.; Kutsch, W.; Longdoz, B.; Rambal, S.; Valentini, R.; Vesala, T.; et al. Towards a Standardized Processing of Net Ecosystem Exchange Measured with Eddy Covariance Technique: Algorithms and Uncertainty Estimation. *Biogeosciences* **2006**, *3* (4), 571−583.
(63) Falge, E.; Baldocchi, D.; Olson, R.; Anthoni, P.; Aubinet, M.; Bernhofer, C.; Burba, G.; Ceulemans, R.; Clement, R.; Dolman, H.; et al. Gap Filling Strategies for Defensible Annual Sums of Net Ecosystem Exchange. *Agric. For. Meteorol.* **2001**, *107* (1), 43−69.
(64) Reichstein, M.; Falge, E.; Baldocchi, D.; Papale, D.; Aubinet, M.; Berbigier, P.; Bernhofer, C.; Buchmann, N.; Gilmanov, T.; Granier, A.; et al. On the Separation of Net Ecosystem Exchange into Assimilation and Ecosystem Respiration: Review and Improved Algorithm. *Glob. Change Biol.* **2005**, *11* (9), 1424−1439.
(65) Foken, Th.; Wichura, B. Tools for Quality Assessment of Surface-Based Flux Measurements. *Agric. For. Meteorol.* **1996**, *78* (1), 83−105.
(66) Kljun, N.; Calanca, P.; Rotach, M. W.; Schmid, H. P. A Simple Two-Dimensional Parameterisation for Flux Footprint Prediction (FFP). *Geosci. Model Dev.* **2015**, *8* (11), 3695−3713.
(67) Spirig, C.; Neftel, A.; Ammann, C.; Dommen, J.; Grabmer, W.; Thielmann, A.; Schaub, A.; Beauchamp, J.; Wisthaler, A.; Hansel, A. Eddy Covariance Flux Measurements of Biogenic VOCs during ECHO 2003 Using Proton Transfer Reaction Mass Spectrometry. *Atmos. Chem. Phys.* **2005**, *5* (2), 465−481.
(68) Wienhold, F. G.; Welling, M.; Harris, G. W. Micrometeorological Measurement and Source Region Analysis of Nitrous Oxide Fluxes from an Agricultural Soil. *Atmos. Environ.* **1995**, *29* (17), 2219−2227.
(69) Geddes, J. A.; Murphy, J. G. Observations of Reactive Nitrogen Oxide Fluxes by Eddy Covariance above Two Midlatitude North American Mixed Hardwood Forests. *Atmos. Chem. Phys.* **2014**, *14* (6), 2939−2957.
(70) Karl, T.; Harley, P.; Guenther, A.; Rasmussen, R.; Baker, B.; Jardine, K.; Nemitz, E. The Bi-Directional Exchange of Oxygenated VOCs between a Loblolly Pine (<I > Pinus Taeda</I>) Plantation and the Atmosphere. *Atmos. Chem. Phys.* **2005**, *5* (11), 3015−3031.
(71) Wolfe, G. M.; Thornton, J. A.; Yatavelli, R. L. N.; McKay, M.; Goldstein, A. H.; LaFranchi, B.; Min, K.-E.; Cohen, R. C. Eddy Covariance Fluxes of Acyl Peroxy Nitrates (PAN, PPN and MPAN) above a Ponderosa Pine Forest. *Atmos. Chem. Phys.* **2009**, *9* (2), 615−634.
(72) Hartmann, W. R.; Santana, M.; Hermoso, M.; Andreae, M. O.; Sanhueza, E. Diurnal Cycles of Formic and Acetic Acids in the Northern Part of the Guayana Shield, Venezuela. *J. Atmos. Chem.* **1991**, *13* (1), 63−72.
(73) Guenther, A.; Hewitt, C. N.; Erickson, D.; Fall, R.; Geron, C.; Graedel, T.; Harley, P.; Klinger, L.; Lerdau, M.; Mckay, W. A.; et al. A Global Model of Natural Volatile Organic Compound Emissions. *J. Geophys. Res.* **1995**, *100* (D5), 8873−8892.
(74) Guenther, A.; Karl, T.; Harley, P.; Wiedinmyer, C.; Palmer, P. I.; Geron, C. Estimates of Global Terrestrial Isoprene Emissions Using MEGAN (Model of Emissions of Gases and Aerosols from Nature). *Atmos. Chem. Phys.* **2006**, *6* (11), 3181−3210.
(75) Kesselmeier, J.; Staudt, M. Biogenic Volatile Organic Compounds (VOC): An Overview on Emission, Physiology and Ecology. *J. Atmos. Chem.* **1999**, *33* (1), 23−88.
(76) Seco, R.; Peñuelas, J.; Filella, I. Short-Chain Oxygenated VOCs: Emission and Uptake by Plants and Atmospheric Sources, Sinks, and Concentrations. *Atmos. Environ.* **2007**, *41* (12), 2477−2499.
(77) Villanueva-Fierro, I.; Popp, C. J.; Martin, R. S. Biogenic Emissions and Ambient Concentrations of Hydrocarbons, Carbonyl Compounds and Organic Acids from Ponderosa Pine and Cottonwood Trees at Rural and Forested Sites in Central New Mexico. *Atmos. Environ.* **2004**, *38* (2), 249−260.
(78) Kesselmeier, J.; Bode, K.; Hofmann, U.; Müller, H.; Schäfer, L.; Wolf, A.; Ciccioli, P.; Brancaleoni, E.; Cecinato, A.; Frattoni, M.; et al. Emission of Short Chained Organic Acids, Aldehydes and Monoterpenes from Quercus Ilex L. and Pinus Pinea L. in Relation to Physiological Activities, Carbon Budget and Emission Algorithms. *Atmos. Environ.* **1997**, *31*, 119−133.
(79) Helmig, D.; Ortega, J.; Guenther, A.; Herrick, J. D.; Geron, C. Sesquiterpene Emissions from Loblolly Pine and Their Potential

DOI: 10.1021/acsearthspacechem.9b00182
ACS Earth Space Chem. 2019, 3, 2017−2032

Contribution to Biogenic Aerosol Formation in the Southeastern US. *Atmos. Environ.* **2006**, *40* (22), 4150−4157.
(80) Insam, H.; Seewald, M. S. A. Volatile Organic Compounds (VOCs) in Soils. *Biol. Fertil. Soils* **2010**, *46* (3), 199−213.
(81) Leff, J. W.; Fierer, N. Volatile Organic Compound (VOC) Emissions from Soil and Litter Samples. *Soil Biol. Biochem.* **2008**, *40* (7), 1629−1636.
(82) Sanhueza, E.; Andreae, M. O. Emission of Formic and Acetic Acids from Tropical Savanna Soils. *Geophys. Res. Lett.* **1991**, *18* (9), 1707−1710.
(83) Gray, C. M.; Monson, R. K.; Fierer, N. Biotic and Abiotic Controls on Biogenic Volatile Organic Compound Fluxes from a Subalpine Forest Floor. *J. Geophys. Res. Biogeosciences* **2014**, *119* (4), 2013JG002575.
(84) Mooney, K. The Disruption of an Ant−Aphid Mutualism Increases the Effect of Birds on Pine Herbivores. *Ecology* **2006**, *87*, 1805−1815.
(85) Conway, J. R. A Field Study of the Nesting Ecology of the Thatching Ant, Formica Obscuripes Forel, at High Altitude in Colorado. *Gt. Basin Nat.* **1996**, *56* (4), 326−332.
(86) Crist, T. O.; Wiens, J. A. The Distribution of Ant Colonies in a Semiarid Landscape: Implications for Community and Ecosystem Processes. *Oikos* **1996**, *76* (2), 301−311.
(87) Jenkin, M. E.; Saunders, S. M.; Pilling, M. J. The Tropospheric Degradation of Volatile Organic Compounds: A Protocol for Mechanism Development. *Atmos. Environ.* **1997**, *31* (1), 81−104.
(88) Saunders, S. M.; Jenkin, M. E.; Derwent, R. G.; Pilling, M. J. Protocol for the Development of the Master Chemical Mechanism, MCM v3 (Part A): Tropospheric Degradation of Non-Aromatic Volatile Organic Compounds. *Atmos. Chem. Phys.* **2003**, *3* (1), 161−180.
(89) Farmer, D. K.; Wooldridge, P. J.; Cohen, R. C. Application of Thermal-Dissociation Laser Induced Fluorescence (TD-LIF) to Measurement of HNO3, ∑alkyl Nitrates, ∑peroxy Nitrates, and NO2 Fluxes Using Eddy Covariance. *Atmos. Chem. Phys.* **2006**, *6* (11), 3471−3486.
(90) Farmer, D. K.; Kimmel, J. R.; Phillips, G.; Docherty, K. S.; Worsnop, D. R.; Sueper, D.; Nemitz, E.; Jimenez, J. L. Eddy Covariance Measurements with High-Resolution Time-of-Flight Aerosol Mass Spectrometry: A New Approach to Chemically Resolved Aerosol Fluxes. *Atmos. Meas. Tech.* **2011**, *4* (6), 1275−1289.
(91) Nemitz, E.; Sutton, M. A. Gas-Particle Interactions above a Dutch Heathland: III. Modelling the Influence of the NH3-HNO3-NH4NO3 Equilibrium on Size-Segregated Particle Fluxes. *Atmos. Chem. Phys.* **2004**, *4* (4), 1025−1045.
(92) Trebs, I.; Lara, L. L.; Zeri, L. M. M.; Gatti, L. V.; Artaxo, P.; Dlugi, R.; Slanina, J.; Andreae, M. O.; Meixner, F. X. Dry and Wet Deposition of Inorganic Nitrogen Compounds to a Tropical Pasture Site (Rondônia, Brazil). *Atmos. Chem. Phys.* **2006**, *6* (2), 447−469.
(93) Bouvier-Brown, N. C.; Schade, G. W.; Misson, L.; Lee, A.; McKay, M.; Goldstein, A. H. Contributions of Biogenic Volatile Organic Compounds to Net Ecosystem Carbon Flux in a Ponderosa Pine Plantation. *Atmos. Environ.* **2012**, *60*, 527−533.
(94) Hunter, J. F.; Day, D. A.; Palm, B. B.; Yatavelli, R. L. N.; Chan, A. W. H.; Kaser, L.; Cappellin, L.; Hayes, P. L.; Cross, E. S.; Carrasquillo, A. J.; et al. Comprehensive Characterization of Atmospheric Organic Carbon at a Forested Site. *Nat. Geosci.* **2017**, *10* (10), 748−753.
(95) Karl, T.; Kaser, L.; Turnipseed, A. Eddy Covariance Measurements of Isoprene and 232-MBO Based on NO+ Time-of-Flight Mass Spectrometry. *Int. J. Mass Spectrom.* **2014**, *365-366*, 15−19.
(96) Fantechi, G.; Jensen, N. R.; Hjorth, J.; Peeters, J. Mechanistic Studies of the Atmospheric Oxidation of Methyl Butenol by OH Radicals, Ozone and NO3 Radicals. *Atmos. Environ.* **1998**, *32* (20), 3547−3556.
(97) Lee, A.; Goldstein, A. H.; Kroll, J. H.; Ng, N. L.; Varutbangkul, V.; Flagan, R. C.; Seinfeld, J. H. Gas-Phase Products and Secondary Aerosol Yields from the Photooxidation of 16 Different Terpenes. *J. Geophys. Res.* **2006**, *111* (D17), D17305.
(98) Lee, A.; Goldstein, A. H.; Keywood, M. D.; Gao, S.; Varutbangkul, V.; Bahreini, R.; Ng, N. L.; Flagan, R. C.; Seinfeld, J. H. Gas-Phase Products and Secondary Aerosol Yields from the Ozonolysis of Ten Different Terpenes. *J. Geophys. Res.* **2006**, *111* (D7), D07302.
(99) Martens, C. S.; Shay, T. J.; Mendlovitz, H. P.; Matross, D. M.; Saleska, S. R.; Wofsy, S. C.; Stephen Woodward, W.; Menton, M. C.; De Moura, J. M. S.; Crill, P. M.; et al. Radon Fluxes in Tropical Forest Ecosystems of Brazilian Amazonia: Night-Time CO2 Net Ecosystem Exchange Derived from Radon and Eddy Covariance Methods. *Glob. Change Biol.* **2004**, *10* (5), 618−629.
(100) Wolfe, G. M.; Cantrell, C.; Kim, S.; Mauldin, R. L., III; Karl, T.; Harley, P.; Turnipseed, A.; Zheng, W.; Flocke, F.; Apel, E. C.; et al. Missing Peroxy Radical Sources within a Summertime Ponderosa Pine Forest. *Atmos. Chem. Phys.* **2014**, *14* (9), 4715−4732.
(101) Wesely, M. L. Parameterization of Surface Resistances to Gaseous Dry Deposition in Regional-Scale Numerical Models. *Atmos. Environ.* **1989**, *23* (6), 1293−1304.
(102) Goldstein, A. H.; McKay, M.; Kurpius, M. R.; Schade, G. W.; Lee, A.; Holzinger, R.; Rasmussen, R. A. Forest Thinning Experiment Confirms Ozone Deposition to Forest Canopy Is Dominated by Reaction with Biogenic VOCs. *Geophys. Res. Lett.* **2004**, *31* (22), L22106.
(103) Atkinson, R.; Arey, J. Gas-Phase Tropospheric Chemistry of Biogenic Volatile Organic Compounds: A Review. *Atmos. Environ.* **2003**, *37*, 197−219.
(104) Bouvier-Brown, N. C.; Goldstein, A. H.; Worton, D. R.; Matross, D. M.; Gilman, J. B.; Kuster, W. C.; Welsh-Bon, D.; Warneke, C.; Gouw, J. A.; de Cahill, T. M.; et al. Methyl Chavicol: Characterization of Its Biogenic Emission Rate, Abundance, and Oxidation Products in the Atmosphere. *Atmos. Chem. Phys.* **2009**, *9* (6), 2061−2074.
(105) Travaini, R.; Martín-Juárez, J.; Lorenzo-Hernando, A.; Bolado-Rodríguez, S. Ozonolysis: An Advantageous Pretreatment for Lignocellulosic Biomass Revisited. *Bioresour. Technol.* **2016**, *199*, 2−12.
(106) Wentworth, G. R.; Murphy, J. G.; Benedict, K. B.; Bangs, E. J.; Collett, J. L., Jr. The Role of Dew as a Night-Time Reservoir and Morning Source for Atmospheric Ammonia. *Atmos. Chem. Phys.* **2016**, *16* (11), 7435−7449.
(107) Eller, A. S. D.; Harley, P.; Monson, R. K. Potential Contribution of Exposed Resin to Ecosystem Emissions of Monoterpenes. *Atmos. Environ.* **2013**, *77*, 440−444.
(108) Wang, Z.-P.; Gu, Q.; Deng, F.-D.; Huang, J.-H.; Megonigal, J. P.; Yu, Q.; Lü, X.-T.; Li, L.-H.; Chang, S.; Zhang, Y.-H.; et al. Methane Emissions from the Trunks of Living Trees on Upland Soils. *New Phytol.* **2016**, *211* (2), 429−439.
(109) Warner, D. L.; Villarreal, S.; McWilliams, K.; Inamdar, S.; Vargas, R. Carbon Dioxide and Methane Fluxes From Tree Stems, Coarse Woody Debris, and Soils in an Upland Temperate Forest. *Ecosystems* **2017**, *20* (6), 1205−1216.

DOI: 10.1021/acsearthspacechem.9b00182
ACS Earth Space Chem. 2019, 3, 2017−2032